Atmos. Chem. Phys., 15, 10701–10721, 2015
www.atmos-chem-phys.net/15/10701/2015/
doi:10.5194/acp-15-10701-2015

Atmospheric Chemistry and Physics
Open Access

Thermodynamics of the formation of sulfuric acid dimers in the binary (H_2SO_4–H_2O) and ternary (H_2SO_4–H_2O–NH_3) system

A. Kürten[1], S. Münch[1], L. Rondo[1], F. Bianchi[2,3], J. Duplissy[4,a], T. Jokinen[5], H. Junninen[5], N. Sarnela[5], S. Schobesberger[5,b], M. Simon[1], M. Sipilä[5], J. Almeida[4], A. Amorim[6], J. Dommen[2], N. M. Donahue[7], E. M. Dunne[8,c], R. C. Flagan[9], A. Franchin[5], J. Kirkby[1,4], A. Kupc[10], V. Makhmutov[11], T. Petäjä[5], A. P. Praplan[2,5,d], F. Riccobono[2,e], G. Steiner[5,12,f], A. Tomé[6], G. Tsagkogeorgas[13], P. E. Wagner[10], D. Wimmer[1,a], U. Baltensperger[2], M. Kulmala[5], D. R. Worsnop[5,14], and J. Curtius[1]

[1]Institute for Atmospheric and Environmental Sciences, Goethe University Frankfurt am Main, Frankfurt am Main, Germany
[2]Laboratory of Atmospheric Chemistry, Paul Scherrer Institute, Villigen, Switzerland
[3]Institute for Atmospheric and Climate Science, ETH Zurich, Zurich, Switzerland
[4]CERN (European Organization for Nuclear Research), Geneva, Switzerland
[5]Department of Physics, University of Helsinki, Helsinki, Finland
[6]Laboratory for Systems, Instrumentation, and Modeling in Science and Technology for Space and the Environment (SIM), University of Lisbon and University of Beira Interior, Lisbon, Portugal
[7]Center for Atmospheric Particle Studies, Carnegie Mellon University, Pittsburgh, USA
[8]School of Earth and Environment, University of Leeds, Leeds, UK
[9]Division of Chemistry and Chemical Engineering, California Institute of Technology, Pasadena, USA
[10]Aerosol Physics and Environmental Physics, University of Vienna, Vienna, Austria
[11]Solar and Cosmic Ray Research Laboratory, Lebedev Physical Institute, Moscow, Russia
[12]Ion Physics and Applied Physics, University of Innsbruck, Innsbruck, Austria
[13]Leibniz Institute for Tropospheric Research, Leipzig, Germany
[14]Aerodyne Research Incorporated, Billerica, MA, USA
[a]now at: Helsinki Institute of Physics, University of Helsinki, Helsinki, Finland
[b]now at: Department of Atmospheric Sciences, University of Washington, Seattle, USA
[c]now at: Finnish Meteorological Institute, Kuopio, Finland
[d]now at: Finnish Meteorological Institute, Helsinki, Finland
[e]now at: Joint Research Centre, European Commission, Ispra, Italy
[f]now at: Faculty of Physics, University of Vienna, Vienna, Austria

Correspondence to: A. Kürten (kuerten@iau.uni-frankfurt.de)

Received: 26 March 2015 – Published in Atmos. Chem. Phys. Discuss.: 18 May 2015
Revised: 2 September 2015 – Accepted: 8 September 2015 – Published: 25 September 2015

Abstract. Sulfuric acid is an important gas influencing atmospheric new particle formation (NPF). Both the binary (H_2SO_4–H_2O) system and the ternary system involving ammonia (H_2SO_4–H_2O–NH_3) may be important in the free troposphere. An essential step in the nucleation of aerosol particles from gas-phase precursors is the formation of a dimer, so an understanding of the thermodynamics of dimer formation over a wide range of atmospheric conditions is essential to describe NPF. We have used the CLOUD chamber to conduct nucleation experiments for these systems at temperatures from 208 to 248 K. Neutral monomer and dimer concentrations of sulfuric acid were measured using a chemical ionization mass spectrometer (CIMS). From these measurements, dimer evaporation rates in the binary system were derived for temperatures of 208 and 223 K. We compare these results to literature data from a previous study that was conducted at higher temperatures but is in good agreement with the present study. For the ternary system the formation of

$H_2SO_4 \cdot NH_3$ is very likely an essential step in the formation of sulfuric acid dimers, which were measured at 210, 223, and 248 K. We estimate the thermodynamic properties (dH and dS) of the $H_2SO_4 \cdot NH_3$ cluster using a simple heuristic model and the measured data. Furthermore, we report the first measurements of large neutral sulfuric acid clusters containing as many as 10 sulfuric acid molecules for the binary system using chemical ionization–atmospheric pressure interface time-of-flight (CI-APi-TOF) mass spectrometry.

1 Introduction

The formation of new particles from the gas phase is a frequent and important process in the atmosphere. Substantial progress has been made in recent years in describing the chemical systems and the mechanisms that could potentially be relevant to atmospheric new particle formation (NPF). Observed atmospheric boundary-layer nucleation rates typically correlate with the concentration of gaseous sulfuric acid (Kulmala et al., 2004; Kuang et al., 2008). Moreover, it is generally accepted that the presence of water vapor enhances nucleation in the binary (H_2SO_4–H_2O) system. However, nucleation under typical ground-level conditions cannot be explained by the binary nucleation of sulfuric acid and water vapor (Kulmala et al., 2004; Kerminen et al., 2010), even if the enhancing effect due to ions is taken into account (Kirkby et al., 2011). Therefore, assuming that sulfuric acid is required for nucleation, at least one additional compound is necessary to stabilize the nucleating clusters (Zhang et al., 2012). Ammonia, amines and highly oxidized organic compounds have been identified in ambient samples or tested in laboratory experiments (Ball et al., 1999; Hanson and Eisele, 2002; Chen et al., 2012; Kulmala et al., 2013). Recent chamber experiments showed that the observed atmospheric boundary-layer nucleation rates can, in principle, be explained by sulfuric acid acting in combination with either amines or the oxidation products from α-pinene (Almeida et al., 2013; Schobesberger et al., 2013; Riccobono et al., 2014).

Nucleation has also frequently been observed in the free troposphere, where the temperature and gas mixture differ from those at the surface (Brock et al., 1995; Weber et al., 1995; Clarke et al., 1999; Lee et al., 2003). An important source for stratospheric particles is the tropical tropopause region, where nucleation-mode particles have been observed. Additionally, new particle formation has also been observed in the free troposphere (Brock et al., 1995; Clarke et al., 1999; Borrmann et al., 2010; Weigel et al., 2011). Due to the volatility and the identification of sulfur in collected particles, it was concluded that binary nucleation contributes to (or dominates) the formation of these particles (Brock et al., 1995). Binary homogenous nucleation also seems to play an important role in forming the mid-stratospheric condensation nuclei layer, although ion-induced binary nucleation cannot be ruled out (Campbell and Deshler, 2014). Several studies provide evidence that ion-induced nucleation may be an important process in the free troposphere (Lee et al., 2003; Lovejoy et al., 2004; Kanawade and Tripathi, 2006; Weigel et al., 2011). These studies suggest that binary nucleation is important on a global scale – especially in regions where very low temperatures prevail, and where the concentrations of stabilizing substances involved in ternary nucleation are low.

Nucleation in the binary system starts with the collision of two hydrated sulfuric acid monomers, which form a dimer (Petäjä et al., 2011). In this study, the notation "dimer" refers to a cluster that contains two sulfuric acid molecules plus an unknown amount of water and, in the ternary system, ammonia. The term monomer refers to clusters with one sulfuric acid, irrespective of whether the cluster also contains ammonia and/or water molecules or not. Unless stated otherwise the terms "monomer" and "dimer" describe the neutral, i.e., uncharged, molecules and clusters. The probability that a dimer will or will not grow larger depends on its evaporation rate as well as its collision rate with monomers and larger clusters. Therefore, it is crucial to know the evaporation rate (or the equilibrium constant) of the sulfuric acid dimer in order to understand and model binary nucleation. Hanson and Lovejoy (2006) measured the dimer equilibrium constant over a temperature range of 232 to 255 K. However, no direct measurements have been performed for lower temperatures. Moreover, evidence exists that ammonia is an important trace gas influencing new particle formation in some regions of the atmosphere (Weber et al., 1998; Chen et al., 2012). Numerous studies using quantum chemical calculations have been conducted to study the cluster thermodynamics for the sulfuric acid–ammonia system (Kurtén et al., 2007; Nadykto and Yu, 2007; Torpo et al., 2007; Ortega et al., 2012; Chon et al., 2014). To our knowledge, however, only very few studies have yet reported experimentally determined dimer concentrations for this system (Hanson and Eisele, 2002; Jen et al., 2014). In order to model NPF for the ternary system involving ammonia, it is essential to better understand the thermodynamics of the clusters involved in the nucleation process. Cluster properties derived from measurements can be used for a comparison with the theoretical studies. Such a comparison provides a consistency check for both the models and the measurements.

Here we present experimentally derived dimer evaporation rates for the binary system (H_2SO_4–H_2O) at temperatures of 208 and 223 K. The measurements of the sulfuric acid monomer and dimer were made with a chemical ionization mass spectrometer (CIMS) at the Cosmics Leaving OUtdoor Droplets (CLOUD) chamber. The data are discussed and compared to previously published dimer evaporation rates for the binary system (Hanson and Lovejoy, 2006). Dimer measurements are also available for the ternary system (H_2SO_4–H_2O–NH_3) at 210, 223, and 248 K and some ammonia mixing ratios ($< \sim 10$ pptv). The thermodynamics (dH and dS) of the $H_2SO_4 \cdot NH_3$ cluster were retrieved

from comparison of the measured monomer and dimer concentrations with those predicted using a simple model. Furthermore, neutral cluster measurements using chemical ionization–atmospheric pressure interface time-of-flight (CI-APi-TOF) mass spectrometry are presented for the binary system at 206 K for clusters containing up to 10 sulfuric acid molecules.

2 Methods

2.1 CLOUD chamber

CIMS monomer and dimer measurements were conducted primarily during the CLOUD5 campaign in October and November 2011. Additional CI-APi-TOF measurements were made during one experiment in November 2012 (CLOUD7). The CLOUD chamber has been described in previous publications (Kirkby et al., 2011; Duplissy et al., 2015). The 26.1 m^3 electropolished stainless-steel chamber provides an ultra-clean environment for studying new particle formation and growth. A well-insulated thermal housing and temperature control allow measurements down to 193 K with a stability of a few hundredths of a degree. For cleaning purposes the chamber can be heated up to 373 K and flushed with ultra-clean air at a high ozone concentration. Pure neutral nucleation was studied by applying a high voltage (±30 kV) to upper and lower transparent field cage electrodes (termed clearing field high voltage, or CFHV, in the following). Sampling ports are located around the mid-plane of the cylindrical chamber, where the clearing field is at 0 V. Grounding the electrodes allows measurements of ion-induced nucleation. In the absence of a clearing field, galactic cosmic rays produce ion pairs at a rate of $\sim 2\,cm^{-3}\,s^{-1}$. Much higher ion pair production rates can be achieved by illuminating a section of the chamber (approximately 1.5 m × 1.5 m) using a defocused pion beam from CERN's Proton Synchrotron (Duplissy et al., 2010). Ultra-clean gas is provided to the chamber by mixing nitrogen and oxygen from cryogenic liquids at a ratio of 79 : 21. Different relative humidities (RH) can be achieved by passing a portion of the dry air through a Nafion humidification system. The temperature and the dew/frost point inside the chamber are monitored continuously; the RH is calculated using the equations given by Murphy and Koop (2005). A fiber optic system (Kupc et al., 2011) feeds UV light into the chamber, which initiates the photolytic production of sulfuric acid when H_2O, O_2, O_3, and SO_2 are present. Two mixing fans continuously stir the air inside the chamber, assuring its homogeneity (Voigtländer et al., 2012).

The CLOUD5 campaign was dedicated to experiments investigating new particle formation at low temperatures (down to ∼ 208 K) for the binary (H_2SO_4–H_2O) and the ternary (H_2SO_4–H_2O–NH_3) systems. The particle formation rates at low temperature will be reported in forthcoming papers; this publication focuses on measurements of the sulfuric acid monomer and the sulfuric acid dimer. One future paper will also focus on the determination of the ammonia mixing ratios at the low temperatures. These were evaluated from a careful characterization of the CLOUD gas system, which delivers ammonia diluted in ultra-clean nitrogen and air to the CLOUD chamber. The gas system was characterized by measurements with a long-path absorption photometer (LOPAP; Bianchi et al., 2012), an ion chromatograph (IC; Praplan et al., 2012) and a proton transfer reaction mass spectrometer (PTR-MS; Norman et al., 2007).

Table 1 gives an overview over the main findings relevant to this study obtained from the two different campaigns.

2.2 CIMS and CI-APi-TOF mass spectrometer

During CLOUD5 a CIMS was used for the measurement of sulfuric acid monomers and dimers (Kürten et al., 2011). Using nitrate ions $NO_3^-(HNO_3)_{x=0-2}$, sulfuric acid can be selectively ionized; detection limits below $10^5\,cm^{-3}$ (referring to the monomer of sulfuric acid) can be reached for short integration times, thereby enabling high time resolution (Eisele and Tanner, 1993; Mauldin et al., 1999; Berresheim et al., 2000). The instrument was calibrated before and after the campaign using a system that produces a known concentration of sulfuric acid (Kürten et al., 2012). In this way, the recorded ion signals – for the primary ions and the reactant ions – can be converted into a concentration of sulfuric acid.

HSO_4^- (the product ion from the sulfuric acid monomer) and $HSO_4^-(H_2SO_4)$ (the product ion from the sulfuric acid dimer) are formed by reactions such as

$$NO_3^-(HNO_3)_x + (H_2SO_4)_{1-2}\cdot X \rightarrow HSO_4^-(H_2SO_4)_{0-1}(HNO_3)_y + (x-y+1)\cdot(HNO_3) + X. \quad \text{(R1)}$$

The compound X is, in most cases, water, but in the case of the ternary system, both experiments and quantum chemical calculations suggest that dimers could also be bound to ammonia (Hanson and Eisele, 2002; Kurtén et al., 2007). Ammonia (or X) is expected to evaporate rapidly after the ionization (Ortega et al., 2014). It should be noted here that even if X did not evaporate after the ionization it would probably be removed in the CIMS collision dissociation chamber (CDC). In the CDC any remaining water molecules are stripped off from the core ions and the $NO_3^-(HNO_3)_{0-2}$ ions yield mostly NO_3^- due to the declustering. Therefore, the monomer and dimer sulfuric acid concentrations are estimated to be

$$[H_2SO_4] = \frac{C}{L_{\text{monomer}}} \cdot \ln\left(1 + \frac{CR_{97}}{CR_{62}}\right), \quad \text{(1a)}$$

$$\left[(H_2SO_4)_2\right] = \frac{C}{L_{\text{dimer}}} \cdot \ln\left(1 + \frac{CR_{195}}{CR_{62}}\right). \quad \text{(1b)}$$

Here, CR denotes the count rate for the primary ions (CR_{62} at m/z 62 for NO_3^-), the HSO_4^- ions (CR_{97} at m/z 97), and

Table 1. Overview over the different conditions, instruments, and main findings relevant to this study from the CLOUD5 and CLOUD7 campaigns.

Campaign	Instruments	Binary system	Ternary system	Main findings
CLOUD5	CIMS, APi-TOF	investigated at 208 and 223 K, RH ∼ 10 to 60 %	investigated at 210, 223, and 248 K, ammonia between ∼ 0.5 and 8 pptv	(a) binary system: ion effect on apparent CIMS dimer measurements (Sect. 3.1) (b) binary system: thermodynamics of sulfuric acid dimers (Sect. 3.3) (c) ternary system: thermodynamics of H_2SO_4•NH_3 cluster (Sects. 3.5 and 3.7)
CLOUD7	CIMS, CI-APi-TOF	investigated at 206 K	not investigated at low temperatures	observation of neutral clusters containing up to 10 sulfuric acid molecules (Sect. 3.4)

the $HSO_4^-(H_2SO_4)$ ions (CR_{195} at m/z 195). The constant C is derived from a calibration and has been evaluated as 1.1×10^{10} cm^{-3} with a typical uncertainty of ∼ 30 % (Kürten et al., 2012). The same calibration constant is used for the monomer and the dimer because it is not possible to calibrate the dimer signal. Since both H_2SO_4 and $(H_2SO_4)_2$ are thought to react with the nitrate ions at the collision limit, this assumption is well justified. The factors L_{monomer} and L_{dimer} take into account the penetration through the sampling line from the CLOUD chamber to the CIMS ion source. A sample flow rate of 7.6 standard liters per minute (L min^{-1}) and a sampling line length of 100 cm were used to calculate the transmission. The diffusion coefficient has been calculated for the respective temperature and RH for the monomer from the data given by Hanson and Eisele (2000). It was assumed that the diffusivity of the hydrated dimer (see Henschel et al., 2012) equals 0.06 ± 0.01 cm^2 s^{-1} at 298 K and varies with temperature as $(298\,\mathrm{K}/T)^{1.75}$.

Some dimer dissociation in the CIMS CDC section cannot be ruled out, although the $HSO_4^-(H_2SO_4)$ ion has a very high bond energy (Curtius et al., 2001). However, as described in the next section, this effect is very likely minor, and, to the extent that it occurs, it is taken into account in the characterization of the dimer detection efficiency.

During the CLOUD7 campaign, sulfuric acid and its clusters were measured with two CI-APi-TOF mass spectrometers (Jokinen et al., 2012; Kürten et al., 2014); the H_2SO_4 monomer was also measured by the CIMS. However, during CLOUD7 it was not possible to measure the dimers with the CIMS due to instrumental problems. The CI-APi-TOF has a chemical ionization source almost identical to the CIMS but which uses a time-of-flight mass spectrometer with high mass resolution (around 4500 Th/Th) and mass accuracy (better than 10 ppm). These features as well as the wide mass range (up to around 2000 Th) enable detection and unambiguous identification of the elemental composition of clusters. As will be shown in Sect. 3.4, neutral clusters containing as many as 10 sulfuric acid molecules were detected during a binary experiment at 206 K.

2.3 Quantification of sulfuric acid dimer concentration

As it is not possible to calibrate the CIMS or the CI-APi-TOF with a known concentration of sulfuric acid dimers, a different method was chosen to allow the quantification of the dimer concentration. To estimate the relative sensitivity towards the dimers (m/z 195) in comparison to the monomer (m/z 97), ion-induced clustering (IIC) during calibration can be evaluated. If the sulfuric acid monomer concentration is large enough, efficient formation of $HSO_4^-(H_2SO_4)$ can occur due to clustering of HSO_4^- and H_2SO_4 within the CIMS ion drift tube (Hanson and Eisele, 2002). The estimated dimer count rate through this process is (Zhao et al., 2010; Chen et al., 2012)

$$\mathrm{CR}_{195,\mathrm{IIC}} = \frac{1}{2}\cdot k_{21}\cdot t_{\mathrm{react}}\cdot \mathrm{CR}_{97}\cdot C\cdot \ln\left(1+\frac{\mathrm{CR}_{97}}{\mathrm{CR}_{62}}\right). \quad (2)$$

The reaction time t_{react} is approximately 50 ms in our case (Kürten et al., 2012). A value of 8×10^{-10} cm^3 s^{-1} was used for k_{21}, the rate constant for reaction between HSO_4^- and H_2SO_4 (Zhao et al., 2010). The measured count rate CR_{195} was compared to the expected count rate during a calibration in which a high concentration of sulfuric acid monomers was presented to the CIMS. From this comparison, we concluded that the dimer signal is suppressed by a factor of 1.2 relative to the monomer signal. The discrepancy can be due to either mass discrimination or to some fragmentation in the CIMS CDC. In any case, it means that the measured dimer signal needs to be multiplied by a factor of 1.2 (with an estimated statistical uncertainty of less than 10 %) when its concentration is evaluated.

The background signal, e.g., from electronic noise, is always subtracted before the dimer concentration is evaluated according to Eq. (1b). The background was obtained by averaging over a certain period just before the experiment started,

i.e., before the UV lights were turned on and the H_2SO_4 was produced. In addition to the background, the contribution from IIC is subtracted from the dimer signal (Chen et al., 2012). This effect becomes relevant at about 1×10^7 cm^{-3} for the sulfuric acid monomer under the conditions of this study.

2.4 Sulfuric acid dimer evaporation rate

The goal of this study is to determine sulfuric acid dimer evaporation rates from data obtained by monomer and dimer measurements. In order to derive a formula for the evaporation rate it is useful to start with the basic equations governing the loss and the production of the clusters. Since low-temperature conditions (208 and 223 K for the binary system) are considered in this study, the assumption is made that only the smallest clusters (dimer and trimer) have appreciable evaporation rates (Hanson and Eisele, 2006). The balance equation for the dimer concentration in this case is

$$\frac{\mathrm{d}N_2}{\mathrm{d}t} = 0.5\cdot G_{1,1}\cdot K_{1,1}\cdot N_1^2 + k_{3,\mathrm{e}}\cdot N_3 - \left(k_{2,\mathrm{w}} + k_{\mathrm{dil}} + \sum_{i=1}^{n} G_{2,i}\cdot K_{2,i}\cdot N_i + k_{2,\mathrm{e}}\right)\cdot N_2, \quad (3)$$

where N_i is the concentration of the cluster containing i sulfuric acid molecules. The evaporation rate $k_{i,\mathrm{e}}$ refers to the evaporation of one sulfuric acid molecule from a cluster containing i sulfuric acid molecules. In a chamber experiment such as CLOUD, three loss processes are relevant for neutral particles; these include the wall loss rate $k_{i,\mathrm{w}}$, the dilution rate k_{dil} through the replenishment of the chamber air (independent of particle size), and coagulation with the coefficient $K_{i,j}$ describing collisions between the clusters i and j. The factor $G_{i,j}$ represents an enhancement in the collision rates due to dipole–dipole interactions (McMurry, 1980; Chan and Mozurkevich, 2001). In order to derive an expression for the dimer evaporation rate, we assume steady state ($\mathrm{d}N_2/\mathrm{d}t = 0$). Equation (3) can then be written as

$$k_{2,\mathrm{e}} = \frac{0.5\cdot G_{1,1}\cdot K_{1,1}\cdot N_1^2}{N_2} + \frac{k_{3,\mathrm{e}}\cdot N_3}{N_2} - \left(k_{2,\mathrm{w}} + k_{\mathrm{dil}} + \sum_{i=1}^{n} G_{2,i}\cdot K_{2,i}\cdot N_i\right). \quad (4)$$

It is useful to estimate the relative importance of the three terms on the right-hand side of Eq. (4). The numerator in the first term describes the production rate of dimers from monomers. The collision constant for two monomers is approximately 2.8×10^{-10} cm^3 s^{-1} at 208 K. If the enhancement factor G due to dipole–dipole interactions is included, this value is $\sim 6.9\times10^{-10}$ cm^3 s^{-1} (McMurry, 1980; Chan and Mozurkevich, 2001). As an example, at 208 K under binary conditions, the smallest monomer concentration evaluated is 2×10^6 cm^{-3}, at which point the dimer was evaluated as 1×10^4 cm^{-3} (Sect. 3.3). These values yield 0.2 s^{-1} for the first term. The second term is significantly smaller than the first term, so it can be neglected due to the reasons listed in the following. The trimer concentration (although it was not measured) should be smaller than the dimer concentration because the trimer is produced from the dimer. Moreover, the trimer evaporation rate is expected to be lower than the dimer evaporation rate (e.g., 1.6×10^{-3} s^{-1} for the trimer, and 0.3 s^{-1} for the dimer at 208 K and 20 % RH; see Hanson and Lovejoy, 2006). The third term includes losses due to walls, dilution, and coagulation. The wall loss rate for a dimer is approximately 1.5×10^{-3} s^{-1}, while loss due to dilution is $\sim 1\times10^{-4}$ s^{-1} (Kürten et al., 2014). The loss due to coagulation depends on the particle size distribution, and can be important when the dimer evaporation rate is small. Loss of dimers due to collisions with monomers (i.e., growth to form trimers) then dominates the coagulation term, which is usually on the order of 10^{-2} s^{-1} (e.g., $N_1 = 1\times10^7$ cm^{-3} and $G_{1,1}\cdot K_{1,1} = 6.9\times10^{-10}$ cm^3 s^{-1}). All elements of the third term are, thus, small compared with the first term, and so these can also be neglected. For the conditions of this study, consistent with the extrapolated data by Hanson and Lovejoy (2006), the evaporation rates are, however, larger than 10^{-2} s^{-1}. This means that evaporation dominates over the other losses; therefore, $k_{2,\mathrm{e}}$ can be approximated by

$$k_{2,\mathrm{e}} = \frac{0.5\cdot G_{1,1}\cdot K_{1,1}\cdot N_1^2}{N_2}. \quad (5)$$

The concentrations used in Eq. (5) are averages over periods when conditions are close to steady state. These periods are defined by conditions where the production and loss rates for the dimer and the monomer are almost identical and the concentrations are not subject to significant changes anymore. If losses by processes other than evaporation were not negligible, retrieval of evaporation rates would require use of a numeric model that also includes larger clusters since coagulation loss depends on concentrations of all other clusters. Nevertheless, model calculations simulating cluster and particle concentrations are needed to evaluate other effects relevant to this study, as will be discussed in the next sections.

Comparison of the rate constants used for the reactions between HSO_4^- and H_2SO_4 (Sect. 2.3) and between H_2SO_4 and H_2SO_4 yields that the neutral–neutral collision rate is about the same as the charged–neutral collision rate. This is due to the relatively large enhancement factor from dipole–dipole interactions for the neutral–neutral rates (McMurry, 1980; Chan and Mozurkevich, 2001) and the observation that the reaction between the bisulfate ion and sulfuric acid seems not to proceed at the collisional rate (Zhao et al., 2010). We have no mechanistic explanation as to why the formation of $HSO_4^-(H_2SO_4)$ should proceed at a rate slower than the collision rate. Comparison with similar ion–molecule reactions shows, for example, that the formation of $NO_3^-(H_2SO_4)$ proceeds at the collision rate (Viggiano et al., 1997), whereas this does not seem to be the case for the formation of

$NO_3^-(HNO_3)$ (Viggiano et al., 1985). Uncertainties regarding the rate of formation for the $HSO_4^-(H_2SO_4)$ cluster remain, and these need to be addressed in future studies. Further discussion about the consequences this uncertainty has on the present study is provided in Sect. 3.8.

2.5 SAWNUC model

The Sulfuric Acid Water NUCleation (SAWNUC) model of Lovejoy et al. (2004) simulates ion-induced nucleation in the binary system. Cluster growth is treated explicitly by a step-by-step addition of sulfuric acid molecules, while equilibrium with water molecules is assumed due to the relatively high concentration and evaporation rate of H_2O compared to H_2SO_4. SAWNUC takes into account sulfuric acid condensation and evaporation, coagulation, and losses due to walls and dilution (Ehrhart and Curtius, 2013). In SAWNUC, evaporation rates of small, negatively charged clusters are based on measured thermodynamics and partly on quantum chemical calculations (Lovejoy and Curtius, 2001; Froyd and Lovejoy, 2003). More detailed information on SAWNUC can be found in Lovejoy et al. (2004), Kazil and Lovejoy (2007), and Ehrhart and Curtius (2013).

As this study focuses on neutral binary nucleation, we neglect the charged-cluster channel and only simulate the neutral channel. Coagulation coefficients have been calculated according to Chan and Mozurkewich (2001). They quantified London–van der Waals forces (dipole–dipole interactions) for particles in the binary system based on the theory by Sceats (1989). Within this study of nucleation at low temperatures, only dimer (and sometimes trimer) evaporation has been taken into account. The exact input parameters are specified in the following sections.

2.6 Dimer transmission through the sampling line

Previous dimer evaporation rates were evaluated with the CIMS ionization source integrated within a temperature-controlled flow tube (Hanson and Lovejoy, 2006). This setup ensured that the temperature did not change between the times when the dimers were formed and when they were ionized. In the present study, the dimers formed inside the CLOUD chamber, which is very precisely temperature-controlled. However, the monomers and dimers had to be transported from the chamber to the CIMS through a 100 cm long sampling line. The first ~ 80 cm of this line was held at the same temperature as the chamber because it protruded through the thermal housing and into the chamber. Moreover, the sampling line was enclosed by an insulated copper tube. Since a large part of the copper volume was placed inside the thermal housing, the cold temperature was maintained over the full length of the copper tube due to efficient heat conduction even for a short section of the tube that was located outside the chamber, while the insulation minimized heat transfer to the surrounding air. The CIMS ion drift tube was connected to the tip of the copper-jacketed sampling line by means of a short tube that was not temperature-controlled, exposing the last 15 to 20 cm (the measured length is closer to 15 cm, but to be conservative we took into account a somewhat longer distance) of the sampling line to warmer temperatures. In this region the dimers could in principle have suffered from evaporation.

To estimate the evaporation effect, a finite-difference method was used to calculate the temperature profile, as well as the dimer concentration across the sampling line over its full length. The differential equations for the monomer ($i = 0$) and dimer ($i = 1$) concentrations c_i were solved as a function of the radial and axial coordinates r and z (Kürten et al., 2012):

$$\frac{\partial c_i}{\partial t} = D_i \cdot \left(\frac{1}{r} \cdot \frac{\partial c_i}{\partial t} + \frac{\partial^2 c_i}{\partial r^2} + \frac{\partial^2 c_i}{\partial z^2}\right) - \frac{2Q}{\pi R^2} \cdot \left(1 - \frac{r^2}{R^2}\right) \cdot \frac{\partial c_i}{\partial z} + s_i, \quad (6)$$

where D_i is the diffusivity, Q is the flow rate, and R is the radius of the tube. A parabolic flow profile was assumed and the geometry was divided into small areas in order to solve the differential equations by a finite-difference method. The source terms s_i include evaporation and production of dimers and loss and production of monomers due to self-coagulation and evaporation of dimers. Further reactions (coagulation with larger clusters/particles) were not taken into account since the time is rather short (< 1 s for $Q = 7.5\,\mathrm{L\,min^{-1}}$, $R = 0.005$ m, and $L = 1$ m) and the other loss terms are dominant. A similar differential equation is used to determine the temperature inside the tube before the concentrations are calculated. This temperature is used to calculate the evaporation of dimers in each of the small areas. The time-dependent equations (time t) are repeatedly solved until a reasonable degree of convergence is reached.

Figure 1 shows the results for a chamber temperature of 223 K. The walls of the first 80 cm of the sampling line were held at 223 K, while those of the last 20 cm were held at 293 K (which was a typical maximum daytime temperature in the experimental hall during the CLOUD5 campaign). It should be noted that this is an extreme case because, in reality, the temperature would slowly approach 293 K over the last 20 cm due to heat conduction along the walls of the sampling line. However, the calculations performed here are used to obtain an upper-bound estimate of the error due to evaporation. The temperature of the walls is indicated in black (223 K) and grey (293 K). Figure 1 shows the normalized concentration of dimers after initializing the monomer concentration to $1 \times 10^7\,\mathrm{cm^{-3}}$; the dimer was assumed to be at equilibrium initially. It was further assumed that both monomers and dimers are lost to the walls due to diffusion, and that at the same time dimers are formed due to collisions of monomers but can also evaporate. Larger clusters or parti-

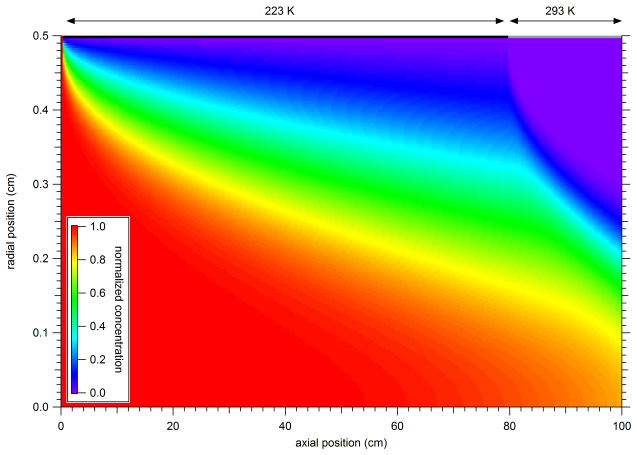

Figure 1. Simulated transmission of dimers through the CIMS sampling line at a temperature of 223 K for the incoming air. The temperature of the sampling line is fixed to 223 K for the first 80 cm (black line along top axis) and to 293 K for the last 20 cm (grey line along top axis). Wall loss is the dominant loss process over the first 80 cm, whereas evaporation is an additional loss process for the last 20 cm. The overall transmission (diffusion loss and evaporation) is 22.8 % at a flow rate of 7.6 L min^{-1}, while it is 47.5 % when evaporation is neglected (diffusion loss only). See text for details.

cles were not taken into account. The dimer evaporation rate as a function of temperature was taken from the literature at this stage (Hanson and Lovejoy, 2006).

The profile shown in Fig. 1 indicates that, during the first 80 cm, dimers are lost primarily via diffusion because, in this section, they are essentially in equilibrium regarding formation and evaporation; only over the last 20 cm does evaporation have an appreciable effect on the dimer concentration. However, only the region close to the walls of the sampling line shows a rise in the gas temperature; the center of the sample flow is essentially unaffected. The estimated overall transmission efficiency for dimers is 0.228 at a flow rate of 7.6 L min^{-1} in the half-inch tube (inner diameter $\sim$ 10 mm). If the temperature were held constant at 223 K over the entire tube length, the transmission would increase to 0.475 because only wall losses would take place. Since the dimer concentration is corrected for the effect of diffusion loss (see Eq. 1b), the additional loss factor due to evaporation would be $(1/0.228)/(1/0.475) = 2.08$. However, this is an upper-bound estimate of the error introduced through evaporation since the temperature is, in reality, gradually changing over the last 20 cm instead of increasing as a step function as simulated. For the lower temperature of 208 K, the effect is even smaller. From the estimations presented in this section it can, therefore, be concluded that, while the sampling conditions are not ideal, the maximum error introduced is very likely smaller than a factor of 2 (see also error discussion in Sect. 3.8).

3 Results and discussion

3.1 Neutral vs. ion-induced experiments

Figure 2 (upper panel) shows the measured monomer and dimer concentrations from a binary experiment at 208 K. The experiment is started when the UV lights are turned on (at 14:16 UTC). The first stage is conducted in a neutral environment with the CFHV enabled. At 16:00 UTC (marked by the dashed vertical line) the electrodes are grounded and galactic cosmic rays (GCRs) lead to a buildup of ions in the chamber. While the monomer concentration is not affected significantly by the GCRs because the small ion concentration is generally only on the order of a couple of thousand (Franchin et al., 2015) and the HSO_4^- ions are not efficiently being detected by the CIMS (Rondo et al., 2014), the dimer concentration is. For the neutral conditions the dimer signal above background is due to neutral $(H_2SO_4)_2$. During the GCR stage of the experiment, the dimer signal gradually increases. This could be due to either neutral dimers being charged in the CIMS or charged dimer ions forming within the CLOUD chamber.

Unfortunately, there was no ion filter installed in the CIMS sampling line during CLOUD5 to eliminate the ion contribution to the CIMS signal. However, evidence exists that the additional signal during GCR conditions is caused by a buildup of chamber ions rather than formation of additional neutral dimers during the ion-induced experiments. Recently, it was reported that HSO_4^- ions clustered to large oxidized organic molecules (OxOrg) can be efficiently detected by the CIMS (Rondo et al., 2014).

When both ions and sufficient H_2SO_4 are present in the chamber, $HSO_4^-(H_2SO_4)_n$ with $n \geq 1$ will be formed (Eisele et al., 2006); these ions are apparently being detected by the CIMS as dimers to some extent. The light HSO_4^- ions will be rapidly lost to the walls of the CIMS sampling line, whereas the larger $HSO_4^-(H_2SO_4)_{n\geq 1}$ ions will have a lower loss rate. Therefore, the larger ions tend to have a higher chance to survive the transport to the CIMS, where they can be eventually detected as artifact dimers. If this were the case, some of the observed dimer signal from the GCR stage in Fig. 2 might not be related to the neutral dimers, and should be discarded.

The atmospheric pressure interface time-of-flight (APi-TOF; Junninen et al., 2010) mass spectrometer measured the ion composition during the first part of the CLOUD5 campaign. Figure 2 (lower panel) shows the $HSO_4^-(H_2SO_4)_n$ ($n = 0$ to 8) cluster ion signals during a binary beam experiment at 223 K. In addition, the apparent CIMS dimer concentration is displayed. The dimer signal is well correlated with the $HSO_4^-(H_2SO_4)_n$ signal for $n \geq 5$ (e.g., Pearson's correlation coefficient between the dimer and the $HSO_4^-(H_2SO_4)_5$ signal is 0.93), indicating that the dimer signal due to ions arises mostly from larger cluster ions (hexamer and larger) which, at least partly, fragment to $HSO_4^-(H_2SO_4)$ before they reach the mass spectrometer. It is, however, not clear whether

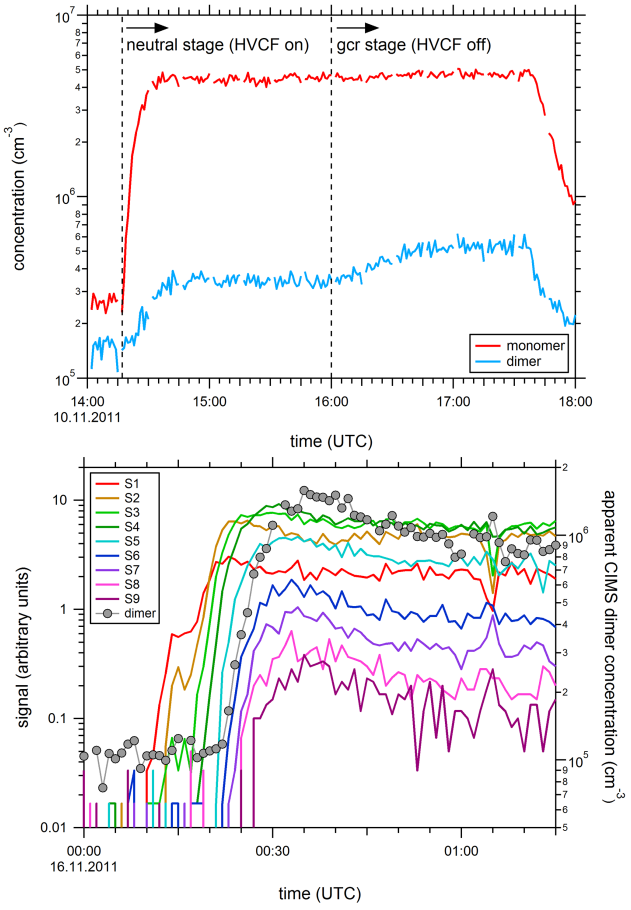

Figure 2. Upper panel: observed ion effect on CIMS sulfuric acid dimer (m/z 195) measurements at 223 K. The first part of the experiment is under neutral conditions, whereas the second part is a GCR run with ions present in the chamber. The increase in the dimer signal during the GCR stage is due to ions detected by the CIMS and not due to neutral dimers. Lower panel: comparison between the APi-TOF signals and the CIMS dimer measurements for a different ion-induced experiment at 223 K. The ion clusters (S6, i.e., $HSO_4^-(H_2SO_4)_5$ and larger) show a clear correlation with the apparent dimer signal, which indicates that fragmented cluster ions contribute to the CIMS dimer measurement (Pearson's correlation coefficient between dimer and S6 is 0.93).

only the relatively large charged clusters fragment, or if only these large clusters reach the mass spectrometer due to an enhanced transmission. The study by Rondo et al. (2014) indicates that ions need to be relatively heavy (or have a low enough electrical mobility) in order to reach the CIMS ion drift region. It is, therefore, also possible that ions that are smaller than the hexamer could, in principle, contribute to the CIMS dimer channel, but since they are not efficiently reaching the CIMS, their contribution is negligible. Either possibility would lead to the large charged clusters contributing to the dimer signal (Fig. 2).

Another interesting observation is that the dimer signal comes mainly from the neutral clusters when ammonia is present in the chamber. Recent publications on the ternary ammonia system investigated at CLOUD have shown that the APi-TOF detects $HSO_4^-(H_2SO_4)_n(NH_3)_m$ with $m \geq 1$ when $n \geq 3$ (Kirkby et al., 2011; Schobesberger et al., 2015). Our findings support the observation that the mixed sulfuric acid ammonia ion clusters are more stable than pure sulfuric acid clusters because they do not seem to fragment to the same extent. As a consequence of the observations discussed in this section, only neutral experiments were considered for the evaluation of the dimer evaporation rates in the binary system.

3.2 Effect of fragmentation during neutral experiments

In the binary system, large cluster ions can fragment and contribute to the measured dimer signal. In this section the maximum error due to the observed fragmentation described in Sect. 3.1 is estimated. For neutral cluster measurements, this process is, however, different from that described in the previous section. Under ion-induced conditions the ions are directly sampled from the CLOUD chamber. Therefore, a relatively low concentration of cluster ions can contribute significantly to the dimer signal because the ionization process in the CIMS drift tube is not needed for their detection.

In a worst-case scenario all cluster ions larger than the dimer (originating from neutral clusters after ionization) would fragment and yield one $HSO_4^-(H_2SO_4)$, thereby increasing the apparent dimer concentration. It is important to note that even a very large charged cluster could only yield one $HSO_4^-(H_2SO_4)$ because the clusters carry only one negative charge. The cluster concentrations (dimer and larger) can be calculated using the SAWNUC model. In any case, the cluster concentrations decrease with increasing size, so the potential contribution decreases with increasing cluster size. Figure 3 provides an upper-bound estimate of the magnitude of this effect. In an example calculation for a temperature of 223 K, a sulfuric acid monomer concentration of 2×10^7 cm^{-3} and dimer and trimer evaporation rates from the literature (Hanson and Lovejoy, 2006) are used, while all other evaporation rates are set to zero. The model yields concentrations for the neutral dimer and all larger clusters. Summing the concentrations from the dimer up to a certain cluster size, and normalizing the sum with the dimer concentration, yields the results shown in Fig. 3, which indicate that the contribution of the larger clusters to the dimer is, at most, a factor of 3 larger than that of the dimers, even as one considers the contributions from very large clusters. Again, in this estimation it is considered that even a large fragmented cluster can contribute only one $HSO_4^-(H_2SO_4)$ because all clusters are singly charged. For this reason the cluster number concentrations are summed and not the number of neutral dimers in a cluster.

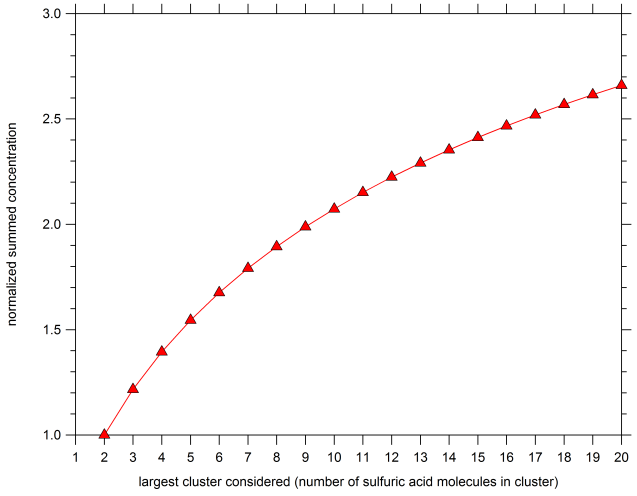

Figure 3. Simulated summed cluster concentrations at 223 K and 20 % RH ($k_{2,e} = 5.8\,s^{-1}$ and $k_{3,e} = 0.056\,s^{-1}$; all larger evaporation rates are zero). The cluster concentrations are summed up to a certain number of sulfuric acid molecules in a cluster starting with the dimer concentration. The values on the x axis indicate the number of sulfuric acid molecules in the largest cluster considered in the summation. All concentrations are normalized by the dimer concentration (at 2×10^7 cm^{-3} monomer concentration).

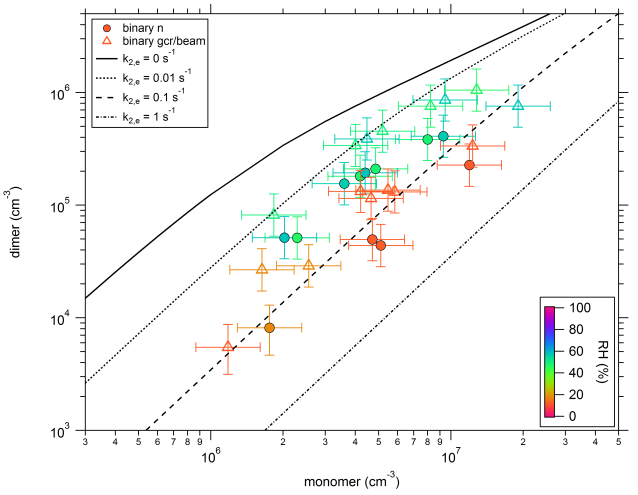

Figure 4. Sulfuric acid dimer concentration as a function of the monomer concentration at 208 K for binary conditions. The full circles are from neutral experiments obtained at steady state and the open triangles from ion-induced experiments. The black lines indicate the modeled dimer concentration for a given dimer evaporation rate with all other cluster evaporation rates set to zero. The color code indicates the relative humidity over supercooled water.

The estimated factor in this section is an upper limit. It is unlikely that all clusters will fragment, or that they always yield $HSO_4^-(H_2SO_4)$ as the product. Instead, HSO_4^- might result from the fragmentation, because, not being an equilibrium process, fragmentation would not always yield the most stable cluster configuration. Moreover, since evaporation cools the cluster, evaporation of neutral sulfuric acid molecules from the largest clusters may be incomplete. Another argument why the data from Fig. 3 provide an upper estimate is due to the reduction in transmission efficiency for the components of the mass spectrometer that is generally observed with increasing mass. In summary, the maximum effect of fragmentation is very likely on the order of a factor of 2, or lower (see also error discussion in Sect. 3.8).

3.3 Binary (H_2SO_4–H_2O) dimer concentrations and evaporation rates

Figure 4 shows the steady-state dimer concentrations as a function of the monomer concentrations at a temperature of 208 K. The data are segregated into binary neutral (solid circles) and ion-induced (open triangles). The color code indicates the relative humidity (RH) over supercooled water. The black lines show the results from the SAWNUC model assuming four different dimer evaporation rates between 0 and 1 s^{-1} (indicated in the legend of the figure). Comparison between the modeled curves and the experimental data gives an indication of the magnitude of the dimer evaporation rates, but the actual values are calculated with Eq. (5) and will be discussed in the context of Fig. 7. While the model curves for 0.1 and 1 s^{-1} are straight lines with a slope of 2 on a log–log plot, the lines for 0 and 0.01 s^{-1} show a pronounced curvature with a slope that approaches a value of one for the high monomer and dimer concentrations. This curvature indicates that a full model calculation would be required in order to derive even smaller evaporation rates than those observed in this study. If the evaporation rate is comparable to the other loss rates, these mechanisms need to be taken into account when estimating $k_{2,e}$. Only when the evaporation rate dominates dimer loss over the full range of $[H_2SO_4]$ can other mechanisms be neglected. The neutral binary data in Fig. 4 indicate that the dimer evaporation rate varies between 0.2 s^{-1} for ∼ 12 % RH and 0.04 s^{-1} for 58 % RH at 208 K. Therefore, relative humidity has a relatively strong effect, one that is more strongly pronounced than the higher-temperature (232 to 255 K) data of Hanson and Lovejoy (2006) suggest (see discussion below). Our signal-to-noise ratio was, however, not high enough to quantify the dimer at temperatures above 223 K for direct comparison. Figure 4 also gives an idea of the magnitude of the ion effect on the CIMS dimer measurements (open triangles). As discussed in Sect. 3.1, the ion-induced binary experiments show systematically higher apparent dimer concentrations than do the neutral experiments. For this reason they are discarded when deriving dimer evaporation rates.

Figure 5 shows the monomer and dimer data for a temperature of 223 K. Again, the data show a pronounced influence of relative humidity. The dimer evaporation rate is approximately 8 s^{-1} at 12 % RH and 0.6 s^{-1} at 50 % RH. The ion

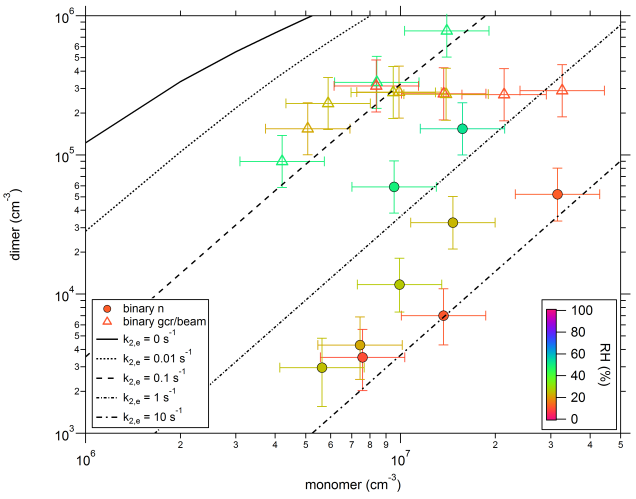

Figure 5. Same as Fig. 4 but for a temperature of 223 K.

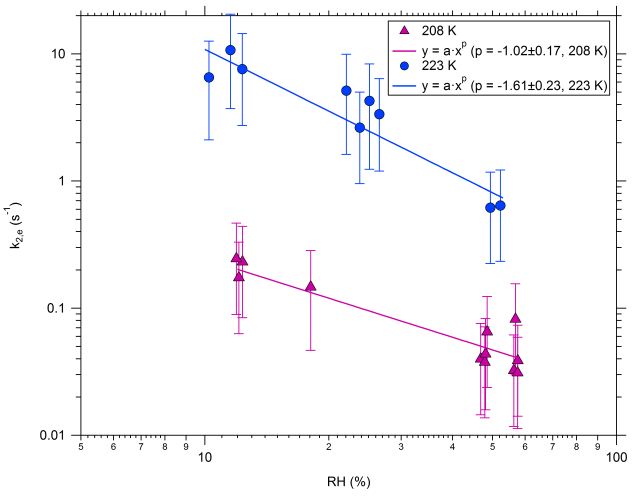

Figure 6. Dimer evaporation rate as a function of the RH for two different temperatures (208 and 223 K). Power law fit curves are shown and the slopes p are indicated in the figure legend.

enhancement effect can be divided into two regimes: one in which it seems to be limited by the availability of sulfuric acid, and a second one in which it is limited by the availability of ions and reaches a plateau where the dimer signal ceases to increase with the sulfuric acid monomer concentration (open triangles).

The evaporation rates derived herein can be compared with the rates reported by Hanson and Lovejoy (2006) after some unit conversions. The equilibrium constant K_{eq} for sulfuric acid dimer formation from monomers in the presence of water has been reported as (Hanson and Lovejoy, 2006)

$$K_{eq} = \frac{p_2}{(p_1)^2} = \frac{1}{\mathrm{Pa}} \cdot \exp\left(\frac{A}{T} - B\right), \quad (7)$$

with $A = (9210 \pm 930)$ K and $B = 31.4 \pm 3.9$ for the temperature, $232 \leq T \leq 255$ K, and a relative humidity of 20 % over supercooled water. Given the reported values for A and B, the thermodynamic properties are estimated to be $\mathrm{d}H = -18.3 \pm 1.8$ kcal mol^{-1} and $\mathrm{d}S = -39.5 \pm 7.8$ cal mol^{-1} K^{-1} (Hanson and Lovejoy, 2006). Equation (7) provides the equilibrium constant in units of Pa^{-1} since the partial pressures p of the monomers and dimers are used. In order to calculate evaporation rates it is necessary to convert the equilibrium constant to units of cm^3 and to further apply the relationship between equilibrium constant, evaporation rate, and collision constant for the dimers (Ortega et al., 2012), leading to

$$k_e = 0.5 \cdot \frac{G_{1,1} \cdot K_{1,1}}{k_B \cdot T \cdot 10^6 \cdot K_{eq}}, \quad (8)$$

where k_B is the Boltzmann constant. We converted equilibrium constants reported by Hanson and Lovejoy (2006) to evaporation rates using Eq. (8). Hanson and Lovejoy (2006) determined evaporation rates at 20 % RH, while our measurements were made at different RHs. Because RH has a significant influence on the dimer evaporation, further analysis is necessary to make the two data sets comparable.

Figure 6 shows the evaluated dimer evaporation rates as a function of the relative humidity (with respect to supercooled water) for two different temperatures (208 and 223 K). The rates from this study are based on the data shown in Figs. 4 and 5 and Eq. (5). The data were fitted by simple power law fits, and the slopes of $p = -1$ (at 208 K) and $p = -1.6$ (at 223 K) indicate that the evaporation rates decrease significantly with increasing RH. Qualitatively this is in agreement with a previous experiment (Hanson and Lovejoy, 2006) and quantum chemical calculations (Ding et al., 2003). However, Hanson and Lovejoy (2006) reported $p = -0.5$, where the exponent p has an uncertainty of ±100 %. Our data indicate a somewhat stronger influence of RH on the evaporation rates, which also seems to be dependent on temperature.

The evaporation rates from Fig. 6 with RH between 10 and 30 % were interpolated to 20 % RH using the reported slopes. Figure 7 shows the data from this study and from Hanson and Lovejoy (2006). Fitting the combined data set for 20 % RH gives the following formulation for the equilibrium constant

$$K_{eq} = \frac{1}{\mathrm{Pa}} \cdot \exp\left(\frac{(10\,109 \pm 609)\ K}{T} - (35.03 \pm 2.61)\right). \quad (9)$$

The black line in Fig. 7 shows the dimer evaporation rates derived from Eq. (9). The uncertainties in Eq. (9) are based on 95 % confidence intervals. Overall, the two data sets are, within errors, consistent with one another, and yield $\mathrm{d}H = -20.1 \pm 1.2$ kcal mol^{-1} and $\mathrm{d}S = -46.7 \pm 5.2$ cal mol^{-1} K^{-1}. We caution that in this study the assumption is made that $\mathrm{d}H$ does not vary with temperature; generally this variation should, however, be small. These data are slightly different than what has been reported by Hanson

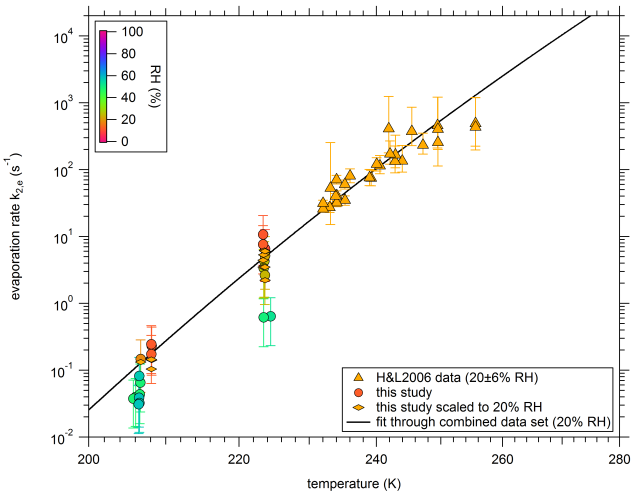

Figure 7. Comparison of the sulfuric acid dimer evaporation rates from this study (circles) and from the literature (triangles; see Hanson and Lovejoy, 2006) as a function of temperature. The color code indicates the relative humidity during the experiments. Diamond symbols represent the data from this study scaled to 20 % RH. The solid line shows a best fit through the data with the thermodynamic properties $\mathrm{d}H = -20.1 \pm 1.2$ kcal mol^{-1} and $\mathrm{d}S = -46.7 \pm 5.2$ cal mol^{-1} K^{-1} at 20 % RH.

and Lovejoy (2006). However, our data agree within errors with results from quantum chemical calculations, taking into account the effect of water vapor (Ding et al., 2003). According to measurements by Hanson and Eisele (2000) and quantum chemical calculations (Temelso et al., 2012; Henschel et al., 2014), the sulfuric acid monomer and dimer can contain water molecules. Therefore, the data from Ding et al. (2003) taking into account the effect of water vapor are relevant for this study. Table 2 shows a comparison between different studies dealing with the sulfuric acid dimer formation. Regarding the effect of water vapor, it should be noted that our experimentally determined evaporation rates represent an average for dimers containing different numbers of water molecules. The exact distribution of water associated with the dimers will be a function of relative humidity and temperature, which cannot be taken into account explicitly in this study. The data by Ding et al. (2003) suggest that almost all sulfuric acid dimers contain four water molecules under the conditions of this study. Therefore, there exist three possibilities for a sulfuric acid monomer ($H_2SO_4(H_2O)_{0-2}$) to dissociate from the dimer with four water molecules. These reactions are listed in the last three rows of Table 2, where the evaporation rates for the monomer of sulfuric acid without water have the highest values. These are about two orders of magnitude faster than the experimentally determined values. One should note, however, that the data by Temelso et al. (2012) indicate a different hydrate distribution and this will have a significant influence on the resulting effective dimer evaporation rate.

3.4 Neutral cluster measurement with CI-APi-TOF in the binary system

During the CLOUD7 campaign, experiments were conducted at ∼ 206 K under binary conditions. In addition to the CIMS, two CI-APi-TOFs were deployed (Jokinen et al., 2012; Kürten et al., 2014). The two instruments are labeled CI-APi-TOF-UFRA (instrument from the University of Frankfurt) and CI-APi-TOF-UHEL (instrument from the University of Helsinki). In contrast to the CIMS used during CLOUD5, the sampling lines of the CI-APi-TOFs were not temperature-controlled. Therefore, dimer evaporation was likely more pronounced. For this reason, we did not attempt to quantify the dimer evaporation rate, although the dimer signals are quantitatively consistent with the data shown in Fig. 3. However, the CI-APi-TOFs have a much wider mass range than the CIMS, i.e., a maximum of approximately 2000 Th. This increased mass range allowed larger clusters to be measured; indeed, neutral sulfuric acid clusters containing up to 10 sulfuric acid molecules, i.e., $HSO_4^-(H_2SO_4)_n$ (n from 0 to 9), were detected (Fig. 8). Eisele and Hanson (2000) previously reported detection of neutral clusters containing up to eight sulfuric acid molecules in a flow-tube experiment using a quadrupole mass spectrometer. However, their measurements were conducted at much higher sulfuric acid concentrations (∼ 10^9 cm^{-3}), whereas in this study the conditions were atmospherically more relevant (sulfuric acid monomer concentration ∼ 1.7×10^7 cm^{-3}). Therefore, the data presented in the following indicate that atmospheric binary nucleation should be directly observable at low temperature, e.g., during aircraft measurements. Water molecules associated with the clusters were not detected with the CI-APi-TOFs; these were most likely evaporated during ion transfer into the high-vacuum section of the instruments. No ammonia was detected in any of the clusters either, even though ammonia can, in principle, be observed with a similar instrument that measures charged clusters (Kirkby et al., 2011), so it can be concluded that the experiment was, indeed, under pure binary conditions.

The upper panel of Fig. 8 shows the time-resolved signals from one of the CI-APi-TOFs ranging from the monomer (HSO_4^-, i.e., S1) up to the decamer ($HSO_4^-(H_2SO_4)_9$, i.e., S10); all of these signals clearly increase following the start of the experiment at 10:02 UTC. From the time-resolved data, the steady-state signals for the different clusters were obtained for both instruments (red and blue symbols in Fig. 8, lower panel). No attempt was made to derive concentrations from the count-rate signals due to the unknown influence of cluster evaporation within the sampling line and transmission within the mass spectrometers. However, the CIMS, which was operated in parallel to the CI-APi-TOFs with its own dedicated sampling line, yielded a monomer concentration of 1.7×10^7 cm^{-3}.

For this experiment we calculated the extent to which ion-induced clustering (IIC) could contribute to the signals. The

Table 2. Thermodynamic properties (dH and dS) and evaporation rates of the sulfuric acid dimer from this study and from the literature.

Study	dH(kcal mol^{-1})	dS(cal mol^{-1} K^{-1})	$k_{2,e}$ at 208 K (s^{-1})	$k_{2,e}$ at 223 K (s^{-1})
This study (20 % RH)	-20.1 ± 1.2	-46.7 ± 5.2	0.15	3.9
Hanson and Lovejoy (20 % RH)	-18.3 ± 1.8	-39.5 ± 7.8	0.32	6.0
$(H_2SO_4)(H_2O) + (H_2SO_4)(H_2O)^*$	−17.8	−48.3	89.3	1550
$(H_2SO_4)(H_2O)_2 + (H_2SO_4)(H_2O)^*$	−21.1	−51.7	0.17	5.0
$(H_2SO_4) + (H_2SO_4)(H_2O)_4^*$	−22.1	−47.3	1.6×10^{-3}	5.7×10^{-2}
$(H_2SO_4)(H_2O) + (H_2SO_4)(H_2O)_3^*$	−22.8	−45.6	1.3×10^{-4}	5.0×10^{-3}
$(H_2SO_4)(H_2O)_2 + (H_2SO_4)(H_2O)_2^*$	−25.6	−55.7	2.4×10^{-5}	1.5×10^{-3}

* Literature data from Ding et al. (2003).

equations provided by Chen et al. (2012) were used to estimate the maximum contribution from IIC (Fig. 8, lower panel). The dashed red line indicates what cluster signals would be expected if all neutral cluster concentrations (dimer and larger) were zero, and the only cluster ions were formed by addition of H_2SO_4 monomers to the HSO_4^- ions within the CIMS drift tube. The large discrepancy between the observations (red diamonds) and the dashed red line (it falls off very steeply with increasing cluster size) shows that the contribution from IIC is negligible. Using SAWNUC together with the dimer and trimer evaporation rates (from this study and from Hanson and Lovejoy, 2006, respectively) allows us to predict all cluster concentrations and then calculate the expected signals (black curve). While the expected signals from the model calculation are substantially higher than the measured ones from the CI-APi-TOF-UFRA, the shape of the black (modeled) and the red (measured) curve is very similar. This suggests that cluster evaporation rates of the trimer and all larger clusters are not high enough to significantly affect their concentrations at this low temperature. The slightly steeper slope of the measurements could be due to a decrease in the detection efficiency as a function of mass of the CI-APi-TOF-UFRA. In this context it is also important to note that the CI-APi-TOF-UFRA was tuned differently than in a previous study (Kürten et al., 2014) in which a relatively steep drop in the sensitivity as a function of mass was observed. The tuning in this study might have led to a more constant detection efficiency as a function of mass. The fact that the measured trimer signal is lower than the tetramer signal is thought to result from fragmentation of the trimers. Similarly, the hexamer appears to suffer some fragmentation. The CI-APi-TOF-UHEL was tuned to maximize the signals in the mass range up to the pentamer. Consequently, in comparison to the other CI-APi-TOF, this led to substantially higher signals in the mass region up to the pentamer, with a pronounced local maximum around the tetramer (blue curve in Fig. 8). However, for the larger masses the signal drops, reaching levels that are comparable to those from the CI-APi-TOF-UFRA.

Because so many questions remain regarding fragmentation, cluster quantification, and the effect of evaporation in the sampling line, the CI-APi-TOF signals are only discussed qualitatively in the present study.

3.5 Sulfuric acid dimer concentrations in the ternary (H_2SO_4–H_2O–NH_3) system

During CLOUD5, ternary nucleation experiments were conducted at temperatures of 210, 223, and 248 K. The addition of relatively small amounts of ammonia (mixing ratios below $\sim$ 10 pptv) led to a significant increase in the sulfuric acid dimer concentrations compared to the binary system, confirming the enhancing effect of ammonia on new particle formation (Ball et al., 1999; Kirkby et al., 2011; Zollner et al., 2012; Jen et al., 2014). In the presence of NH_3, a fraction of the sulfuric acid will be bound to ammonia. However, we assume that the sulfuric acid monomers and dimers will still be ionized by the nitrate primary ions at the same rate as the pure compounds. The ammonia will, however, evaporate very rapidly after the ionization (Hanson and Eisele, 2002). For this reason it is not possible to determine directly the fractions of either the sulfuric acid monomer or the dimer that contains ammonia. Therefore, in the following we assume that the measured monomer is the sum of the pure sulfuric acid monomer and the sulfuric acid monomer bound to ammonia; the same assumption is made for the dimer. It has been suggested that the sensitivity of a nitrate CIMS regarding the sulfuric acid measurements could be affected by the presence of ammonia (or other bases like dimethylamine), which cluster with sulfuric acid (Kurtén et al., 2011; Kupiainen-Määttä et al., 2013). However, recent measurements at the CLOUD chamber indicate that this is very likely a minor affect (Rondo et al., 2015).

Figure 9 shows the measured sulfuric acid dimer concentration as a function of the sulfuric acid monomer concentration for three different temperatures (210, 223, and 248 K), as well as several ammonia mixing ratios ($< \sim$ 10 pptv) under ternary conditions. Two limiting cases that bracket the possible dimer concentrations and the influence of ammonia are indicated by the solid black line and the dashed black line. The solid black line shows the case in which all evaporation rates are set to zero in the SAWNUC model (the kinetic

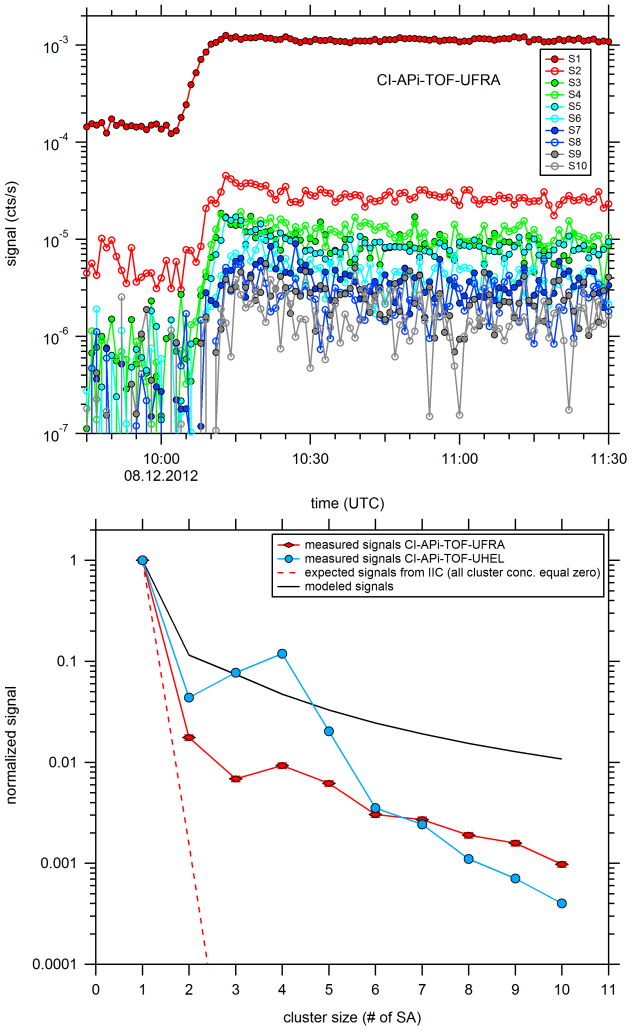

Figure 8. Cluster measurements for the binary system at 206 K and an RH close to 100 % over ice measured with two CI-APi-TOFs (UFRA and UHEL instruments). The upper panel shows the monomer (S1) and the cluster signals (Si, $i \geq 2$) normalized by the nitrate ion signals as a function of time (1 min time resolution) for the CI-APi-TOF-UFRA. The lower panel shows the measured steady-state signals as well as expected signals using different assumptions as function of the cluster size. See text for details.

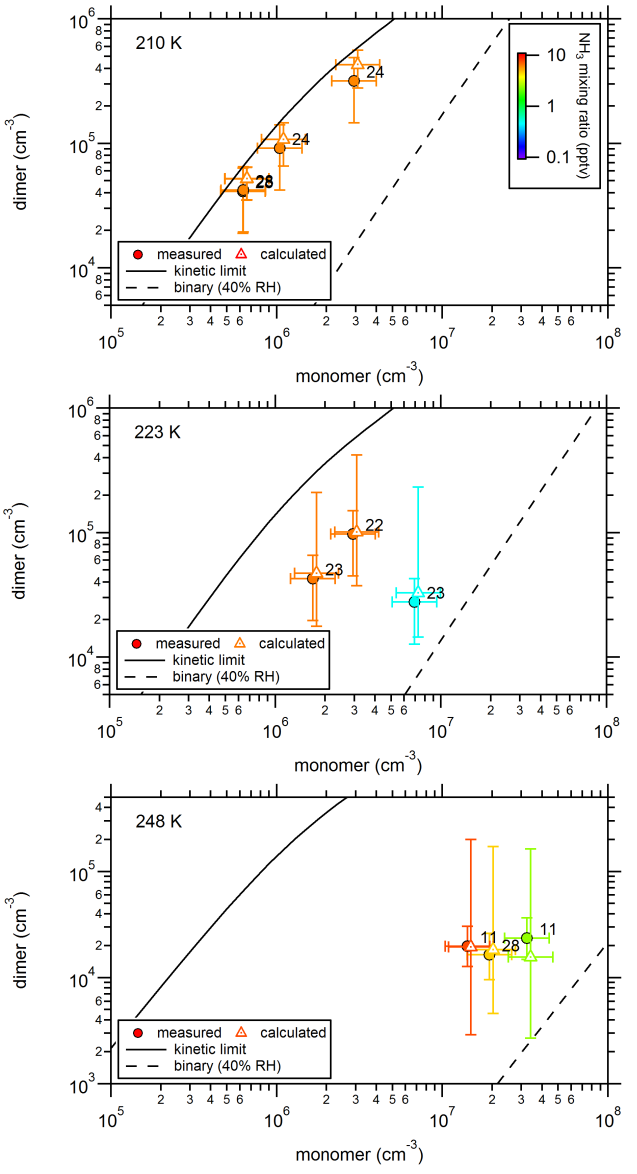

Figure 9. Sulfuric acid dimer concentrations as a function of the sulfuric acid monomer concentration at three different temperatures for the ternary system involving ammonia (ammonia mixing ratio indicated by the color code). The colored circles are the measured concentrations. Lines are from model calculations indicating the expected concentrations for the binary system (dashed line) and the kinetic limit (solid line). The numbers indicate the RH (in %) during an experiment. Open colored triangles are the simulated dimer concentrations using the reaction scheme from Fig. 10. These are slightly offset to the right in order to improve readability.

limit); the dashed black line indicates the case for binary conditions at 40 % RH. It can be seen that, at the lowest temperature (210 K), the dimer concentrations are close to the expected concentrations for kinetically limited cluster formation, as has been previously reported for the ternary sulfuric acid, water, and dimethylamine system at 278 K (Kürten et al., 2014). The ammonia mixing ratio is ∼ 6 pptv in this case (Fig. 9, upper panel). At 223 K two different ammonia mixing ratios were investigated. It can clearly be seen that the dimer concentrations increase with increasing ammonia mixing ratio. Different ammonia mixing ratios (∼ 2.5 to 8 pptv) were also studied at 248 K, but in this case the variation in the ammonia concentration was smaller than for 223 K; therefore, the dimer concentration variation is also less pronounced. In addition, the relative humidity changed from experiment to experiment (RH is indicated by the small numbers written next to the data points); it apparently influenced the dimer concentration, which is not surprising given the re-

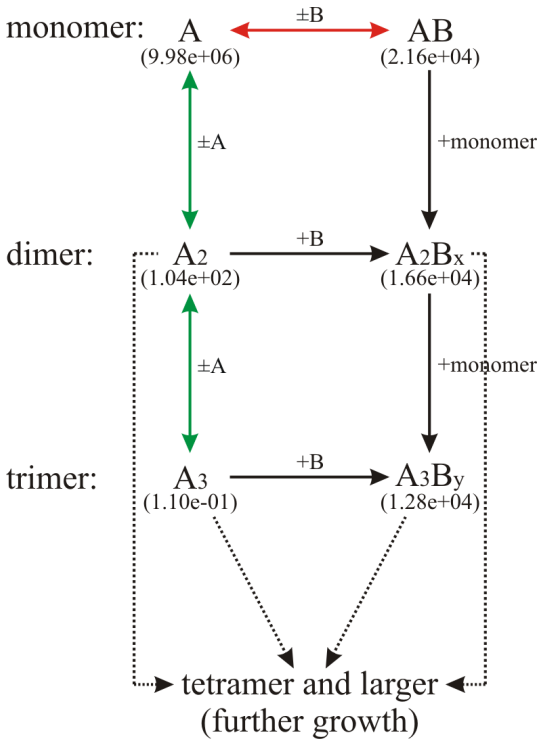

Figure 10. Reaction scheme for the sulfuric acid dimer formation in the ternary system at a low temperature. "A" denotes a sulfuric acid molecule, and "B" an ammonia molecule. "Monomer" is the sum of the concentration of the pure sulfuric acid (A) and the sulfuric acid bound to an ammonia (AB). "Dimer" is the sum of all clusters containing two sulfuric acid molecules (A_2+ A_2B + A_2B_2) and the same applies for the "trimer" with three sulfuric acid molecules. The arrows indicate the relevant reactions and whether only collisional growth (single-ended arrow) or growth as well as evaporation (double-ended arrow) is important. Losses due to walls, dilution, and coagulation are included in the model but not indicated. Small numbers represent concentrations for an example calculation at a temperature of 248 K, a [monomer] of 1×10^7 cm^{-3}, and a [NH_3] of 2×10^8 cm^{-3}. See text for details.

sults described in Sect. 3.3 and those of Hanson and Lovejoy (2006). Our data show that very small ammonia mixing ratios (pptv range) can strongly enhance dimer formation under atmospherically relevant sulfuric acid concentrations and low temperatures.

3.6 Acid–base model

In order to better understand what influences the dimer concentration in the ternary system, we have developed a simple model (Fig. 10). This heuristic model is motivated by recent studies which have simulated acid–base nucleation of sulfuric acid, ammonia, and amines with similar methods, i.e., without simulating every possible cluster configuration explicitly (Chen et al., 2012; Paasonen et al., 2012; Jen et al., 2014). Following the notation of Chen et al. (2012), a sulfuric acid molecule is termed A, while the base ammonia is termed B. Dimers (A_2 or A_2B) may form via two different routes: (a) two sulfuric acid molecules A can collide and form a pure sulfuric acid dimer (A_2), which can further collide with B and form A_2B, or (b) a sulfuric acid molecule can collide with an ammonia molecule and form an AB cluster, which can further collide with A (or another AB cluster) to form A_2B (or A_2B_2). The model further assumes that trimers either can contain solely sulfuric acid (A_3) or are associated with ammonia (A_3B_x).

For all larger clusters we make no distinction between pure sulfuric acid clusters and ammonia-containing clusters. We further assume that the clusters cannot contain more bases than acids, so reactions like AB + B are not considered, as the extra base is expected to evaporate much more rapidly than it can be gained through collisions at the relatively low base concentrations (Schobesberger et al., 2015).

The model differs somewhat from that used by Chen et al. (2012) and Jen et al. (2014). They considered two separate schemes; in their first scheme, they assumed that two different dimer versions exist – a volatile dimer and a less volatile dimer that is formed through collision between the volatile dimer and a base molecule. The less volatile dimer can form a trimer or a tetramer (through self-coagulation), both of which are assumed to be stable. This scheme is similar to pathway (a) described above. Their second scheme assumes that the sulfuric acid monomer can form a cluster AB, which can be turned into a stable dimer. This dimer can then form a trimer that is allowed to evaporate at a rather slow rate (0.4 s^{-1} at 300 K). Once the size of the tetramer is reached the cluster is assumed to be stable. Except for the evaporation rate of the base-containing trimer, this scheme is identical to route (b) described above. Our approach combines the two channels because it seems likely that dimers can be formed through the two different pathways at the same time (Fig. 10), especially when the temperature is low and the evaporation of A_2 is relatively slow. In addition, we assume that the only base-containing cluster that can still evaporate at these low temperatures (248 K and colder) is AB. Quantum chemical calculations (Ortega et al., 2012) and the measurements of Hanson and Eisele (2002) support the assumption that the cluster containing two sulfuric acid molecules and one ammonia molecule is stable even at relatively high temperature (275 K in the Hanson and Eisele, 2002, study). Furthermore, since the evaporation rate of the base-containing trimer reported by Chen et al. (2012) is quite small at 300 K (0.4 s^{-1}), we assume that, at the very low temperatures of this study, this evaporation rate becomes negligible.

The quantum chemistry data from Ortega et al. (2012) support the assumption that a trimer containing at least two bases is relatively stable (evaporation rate below 0.1 s^{-1} at 300 K). However, it predicts that the trimer containing only one ammonia molecule has a high evaporation rate regarding an acid molecule ($\sim$ 1000 s^{-1} at 300 K); additional ammonia in the trimer will lower the evaporation rates. For this reason the

trimer concentration will strongly depend on the ammonia concentration, which controls the cluster distribution. Therefore, the Chen et al. (2012) value can be regarded as a best estimate for the overall trimer evaporation rate for their experimental conditions. Herb et al. (2011) also simulated the effect that one water molecule has on the acid evaporation rate from $(H_2SO_4)_3(NH_3)_1(H_2O)_{0,1}$ clusters. While the water molecule lowers the evaporation rate, the absolute evaporation rate is higher ($2.9 \times 10^4\,s^{-1}$ at 300 K) than for the Ortega et al. (2012) data.

3.7 Thermodynamics of the H_2SO_4•NH_3 cluster

Under these assumptions, the model of Fig. 10 was used to probe the kinetics using the measured sulfuric acid monomer, and ammonia concentrations, along with the dimer (A_2) and trimer (A_3) evaporation rates as a function of relative humidity and temperature from this study and from Hanson and Lovejoy (2006). The only free parameter in the model is then the evaporation rate of AB; we adjusted this until the modeled dimer concentration matched the measured one under steady-state conditions. From the evaporation rates at the different temperatures the thermodynamics (dH and dS) of the cluster AB were retrieved from a least-squares linear fit (logarithm of the equilibrium constant vs. the inverse temperature), which yields $dH = -16.1 \pm 0.6\,kcal\,mol^{-1}$ and $dS = -26.4 \pm 2.6\,cal\,mol^{-1}\,K^{-1}$ for H_2SO_4•NH_3.

Unfortunately, the number of data points used to derive the dH and dS values is quite small. At 210 K the measured dimer concentrations are very close to the kinetic limit estimation, so the evaporation rates must be very low. This indicates that small variations in the monomer and dimer concentration can lead to a large variation in the evaporation rate of AB. These data points were, therefore, neglected. On the other hand, the effect of the relative humidity on the evaporation rates of ammonia-containing clusters is not known, so only those experiments that were conducted at similar RH, i.e., ∼ 25 %, were considered.

Figure 9 also shows the calculated dimer concentrations using the model with the evaporation rate of AB inferred using the derived thermodynamics (open colored triangles). The error bars reflect a variation in the evaporation rate for H_2SO_4•NH_3 according to the uncertainties of the dH and dS values. The lowest dimer concentrations result if the error of dH is implemented in the positive direction and the error of dS in the negative direction. The highest dimer concentrations result by reversing the signs in the error calculation. The good agreement between measured and modeled values indicates that the model successfully reproduces the dimer concentrations over a wide range of conditions. Furthermore, we have also simulated the experiments of Hanson and Eisele (2002) for the ternary system involving ammonia, who used a sulfuric acid concentration of $1.9 \times 10^9\,cm^{-3}$ and an ammonia concentration of $3.8 \times 10^9\,cm^{-3}$ at a temperature of 265 K and an RH of ∼ 10 %. Our calculated dimer concentration agrees with their measured concentration within about 40 %. Table 3 shows a comparison with the cluster concentrations (dimer to pentamer) measured by Hanson and Eisele (2002) and the ones from this study using the acid–base model described above.

Table 4 compares our dH and dS values as well as the corresponding evaporation rates for selected temperatures with other data obtained from quantum chemical calculations (Torpo et al., 2007; Nadykto and Yu, 2007; Ortega et al., 2012; Chon et al., 2014) and from one flow tube experiment (Jen et al., 2014). Overall, the agreement is good. However, it is difficult to take into account the effect the model assumptions have on the outcome of the values from our study. In addition, only a small number of data points have been taken into account in this study.

One also needs to keep in mind that the cluster formation was observed at ∼ 25 % RH (with respect to supercooled water) in this study, while most of the theoretical studies did not take into account the effect of water except the one by Nadykto and Yu (2007). Their data suggest that the evaporation rate of H_2SO_4•NH_3•$(H_2O)_x$ increases when the number of associated water molecules increase. The study by Henschel et al. (2014) indicates that about one water molecule is attached for the RH relevant to this study. However, Henschel et al. (2014) reported their results only for a temperature of 298 K, whereas the temperature of this study is 248 K and lower. Whether the evaporation rate is increasing with increasing RH cannot be concluded from our data; however, one needs to keep in mind that, similar to the dimer in the binary system, the reported evaporation rates and thermodynamic data for the H_2SO_4•NH_3 represent average values that can include clusters with attached water molecules.

The comparison in Table 4 also lists the experimental study by Jen et al. (2014), who determined the evaporation rate of H_2SO_4•NH_3 at ∼ 300 K from a transient version of their second scheme (formation of dimers only via AB; see above). The extrapolated value from the present study is, however, in relatively good agreement with their value. The somewhat lower evaporation rate of Jen et al. (2014) could be explained by the fact that they did not consider the formation of dimers by self-coagulation of A. Furthermore, they assumed that the trimer has an evaporation rate of $0.4\,s^{-1}$. Both these assumptions require a slower evaporation rate for AB than our study suggests to explain the measured dimer concentrations at a given monomer and base concentration.

Overall, our measurements in the ternary system yield values of the thermodynamic properties of the H_2SO_4•NH_3 cluster that are in rather good agreement with the results from quantum chemical calculations. However, since the number of data points is limited, the uncertainty is rather high.

3.8 Uncertainties

The error bars shown in Figs. 4 and 5 include the standard variation in the individual data points and a 30 % (50 %) sys-

Table 3. Comparison between measured cluster concentrations by Hanson and Eisele (2002) and simulated cluster concentrations using the acid–base model described in Sect. 3.6.

Cluster	Hanson and Eisele (2002)	Acid–base model, this study
N_2 (total dimer)	1.1×10^7 cm^{-3}	7.0×10^6 cm^{-3} (−36 %)
N_3 (total trimer)	6.5×10^6 cm^{-3}	5.6×10^6 cm^{-3} (−14 %)
N_4 (total tetramer)	6.6×10^6 cm^{-3}	4.7×10^6 cm^{-3} (−29 %)
N_5 (total pentamer)	$\sim 4 \times 10^6$ cm^{-3}	4.1×10^6 cm^{-3}

Table 4. Thermodynamic properties (dH and dS) and evaporation rates of the H_2SO_4•NH_3 cluster from this study and from the literature.

Study	dH (kcal mol^{-1})	dS (cal mol^{-1} K^{-1})	k_e at 210 K (s^{-1})	k_e at 248 K (s^{-1})	k_e at 300 K (s^{-1})
This study[a]	-16.1 ± 0.6	-26.4 ± 2.6	0.11	36	9.8×10^3
Torpo et al. (2007)[b]	−15.81	−28.57	0.63	200	4.7×10^4
Nadykto and Yu (2007)[b]	−16.72	−30.01	0.15	64	2.1×10^4
Nadykto and Yu (2007), $H_2SO_4(H_2O) + NH_3$	−15.91	−30.23	1.1	370	9.2×10^4
Nadykto and Yu (2007), $H_2SO_4(H_2O)_2 + NH_3$	−15.27	−30.49	6.0	1.5×10^3	3.1×10^5
Nadykto and Yu (2007), $H_2SO_4(H_2O)_3 + NH_3$	−15.44	−32.30	10	2.7×10^3	5.8×10^5
Ortega et al. (2012)[b]	−16.00	−28.14	0.32	107	2.8×10^4
Chon et al. (2014)[b]	−15.43	−29.63	2.7	720	1.5×10^5
Jen et al. (2014)[c]	–	–	–	–	400 to 2500

[a] Experiments conducted at ∼ 25 % RH (with respect to supercooled water). [b] No effect of water vapor considered. [c] Experiment conducted at ∼ 30 % RH.

tematic uncertainty in the monomer (dimer) concentration. The two error components are added together in quadrature. The systematic errors are estimated based on the uncertainties in the calibration coefficient C for the monomer. Due to the higher uncertainty of the sampling losses for the dimer and the uncertainty of the transmission correction factor (Sect. 2.3), a somewhat higher uncertainty has been chosen in comparison to the monomer. The error bars in Fig. 7 are obtained when using Gaussian error propagation on Eq. (5) for the monomer and the dimer concentration.

In addition to these errors, the effects of evaporation of the dimer in the sampling line (Sect. 2.6) and fragmentation (Sect. 3.2) have been discussed above. Each of these effects is very likely on the order of a factor of 2 or smaller. These processes probably influence all of the dimer data to some extent. However, these errors work in opposite directions: evaporation will lead to a reduction of the dimer concentration, while fragmentation of larger clusters will tend to increase the apparent concentration. Therefore, the two effects partially compensate for each other, so they were not taken into account in the calculation of the error bars.

One additional uncertainty is introduced by the assumption that the CIMS detection efficiency is independent of temperature. The study of Viggiano et al. (1997) indicates that the collision rate between nitrate primary ions and sulfuric acid is only a weak function of temperature between 200 and 300 K. Therefore, we expect that temperature only has a small effect on the sulfuric acid concentrations.

The exact values of dimer evaporation rates depend on the choice of $G_{1,1} \cdot K_{1,1}$, i.e., on the overall collision rate between two neutral dimers, and is therefore subject to an additional uncertainty because this value is based on theoretical calculations. However, the thermodynamic data derived in this study do not depend on the value of $G_{1,1} \cdot K_{1,1}$ because both the data from this study and the one from Hanson and Lovejoy (2006) in Fig. 7 were calculated using the same factors. Therefore, when deriving dH and dS, the collision rate cancels out in the calculations (see Eqs. 5 and 8).

In contrast to the exact value of $G_{1,1} \cdot K_{1,1}$ the charged–neutral collision rate k_{21} between HSO_4^- and H_2SO_4 is important because its value scales the dimer concentrations and evaporation rates from this study while leaving the data from Hanson and Lovejoy (2006) unaffected. The reported value of 8×10^{-10} cm^3 s^{-1} for k_{21} from Zhao et al. (2010) suggests that this charged–neutral reaction is not proceeding at the collision limit (value of $\sim 2 \times 10^{-9}$ cm^3 s^{-1}). When using the faster reaction rate for the charged–neutral collision limit, some of the dimer concentrations would exceed the kinetic limit (see Fig. 9, upper panel) because all dimer concentrations would need to be scaled up by a factor of 2.5; therefore the faster rate seems to be implausible. However, using the upper limit for the collision rate results in d$H = -23.0 \pm 1.6$ kcal mol^{-1} and d$S = -58.5 \pm 6.9$ cal mol^{-1} K^{-1}.

The estimates of the thermodynamic properties of the H_2SO_4•NH_3 cluster rely on the assumptions made in the

model (Sect. 3.6). One of the important assumptions made is that the base-containing trimer and tetramer do not evaporate significantly. The data of Ortega et al. (2012) suggest that the evaporation rates of the A_3B_1 and the A_4B_1 clusters are not negligible, even at temperatures at and below 248 K. However, the presence of further ammonia molecules in the trimer and tetramer can lower the evaporation rates and water should have a similar effect (Ortega et al., 2012; Herb et al., 2011). In contrast, the base-containing dimer (A_2B) has a very small evaporation rate. No experimental data have been found that support the relatively high evaporation rates of the base-containing trimer and tetramer. Instead, the study by Hanson and Eisele (2002) concluded that the critical cluster in the H_2SO_4–H_2O–NH_3 system very likely contains two sulfuric acid molecules and one ammonia molecule at temperatures up to 275 K. In addition, an evaporation rate of $0.4\,s^{-1}$ for the base-containing trimer could explain observed atmospheric nucleation rates at relatively warm temperatures of 300 K (Chen et al., 2012). This evaporation rate should decrease further at lower temperatures. Significant uncertainties remain regarding the evaporation rates of these clusters; further experiments will be needed to reduce these in the future.

4 Summary and conclusions

A chemical ionization mass spectrometer (CIMS) was used to measure the concentrations of the neutral sulfuric acid monomer and dimer during nucleation experiments at the CLOUD chamber. These experiments were conducted at temperatures as low as 208 K, making them relevant to conditions in the free troposphere. Both the binary (H_2SO_4–H_2O) system and the ternary system involving ammonia (H_2SO_4–H_2O–NH_3) were investigated.

Comparison of neutral and ion-induced nucleation experiments indicates that the CIMS detected a significant number of fragmented ion clusters. This confirms the so called "ion effect" on the CIMS measurements that was recently described by Rondo et al. (2014). However, while Rondo et al. (2014) observed that fragmented HSO_4^-•OxOrg clusters contributed to the CIMS sulfuric acid monomer measurement, we observed a similar effect for the CIMS sulfuric acid dimer measurement (m/z 195). Interestingly, the ion effect on the CIMS dimers was almost absent as soon as ammonia was present in the CLOUD chamber. This is consistent with the observation that ammonia stabilizes sulfuric acid clusters and thereby enhances nucleation (Kirkby et al., 2011; Schobesberger et al., 2015).

From the measured monomer and dimer signals dimer evaporation rates were derived and compared to previous flow tube measurements made by Hanson and Lovejoy (2006) for the binary system. Their measurements were performed over a temperature range of 232 to 255 K. The data from the present study were obtained at lower temperatures, 208 and 223 K. Together, the two data sets yield a revised version of the Hanson and Lovejoy (2006) formulation for the dimer equilibrium constant at 20 % RH with $\mathrm{d}H = -20.1 \pm 1.2\,\mathrm{kcal\,mol^{-1}}$ and $\mathrm{d}S = -46.7 \pm 5.2\,\mathrm{cal\,mol^{-1}\,K^{-1}}$. This result is obtained when assuming that the evaporation of larger sulfuric acid clusters (trimer and larger) does not contribute significantly to the dimer concentration, which is the case for the conditions of this study. Due to the wide temperature range (208 to 255 K) covered by the two data sets, this new estimate provides a high degree of confidence when being used at the very low temperatures where binary nucleation can be efficient. Regarding the formation of dimers in the binary system Hanson and Lovejoy (2006) stated that an increase in the relative humidity leads to an increase in the dimer equilibrium constant ($K_p \sim RH^p$) with a power dependency of p between 0 and 1. The best estimate for the power dependency was reported to be 0.5 (Hanson and Lovejoy, 2006). Our data indicate that the exponent is around 1 at 208 K and around 1.6 at 223 K, i.e., at the upper end of what has been previously assumed.

The ternary experiments involving ammonia (H_2SO_4–H_2O–NH_3) showed that the addition of very small amounts of ammonia (in the pptv range) strongly enhances the sulfuric acid dimer concentration. The dimer concentrations are systematically higher than those for the binary system at a given temperature and sulfuric acid monomer concentration. Furthermore, they increase with increasing ammonia mixing ratio. This confirms previous suggestions that ammonia acts as a stabilizing agent, even for the very small sulfuric acid clusters. In contrast to the previous experiments, the present results were obtained at atmospherically relevant concentrations of sulfuric acid and ammonia, and at low temperature. For the first time the thermodynamics of the H_2SO_4•NH_3 cluster were experimentally investigated from measurements of the monomer and the dimer. The measurements were made at temperatures of 210, 223, and 248 K, with ammonia mixing ratios below ~ 10 pptv. Using a revised version of a simple conceptual model first proposed by Chen et al. (2012) we were able to derive the thermodynamic properties of the H_2SO_4•NH_3 cluster. The obtained values of $\mathrm{d}H = -16.1 \pm 0.6\,\mathrm{kcal\,mol^{-1}}$ and $\mathrm{d}S = -26.4 \pm 2.6\,\mathrm{cal\,mol^{-1}\,K^{-1}}$ are in good agreement with results from quantum chemical calculations. Using the proposed model with the evaporation rate of the H_2SO_4•NH_3 cluster as a fitting parameter, the measured dimer concentrations in the ternary system can be reproduced with a high accuracy for the conditions of this study. A previous study suggested that the $(H_2SO_4)_2$•NH_3 cluster is thermodynamically stable (Hanson and Eisele, 2002). With this observation, the model can be used to calculate nucleation rates in the ternary system, which relies on experimentally determined thermochemical data and on the assumptions that ammonia-containing trimers and tetramers have insignificant evaporation rates for the conditions of this study.

Finally, large neutral sulfuric acid clusters containing as many as 10 sulfuric acid molecules were observed for the binary system at 206 K. These clusters were measured with two chemical ionization–atmospheric pressure interface time-of-flight (CI-APi-TOF) mass spectrometers. Since these measurements were not made with a temperature-controlled sampling line, the absolute determination of the cluster concentrations was not attempted. However, the signals are consistent with the assumption that cluster growth is essentially kinetically controlled for all of the observed clusters above the dimer. The observation of these large clusters at the upper end of atmospherically relevant sulfuric acid monomer concentration of $\sim 1.7 \times 10^7$ cm^{-3} shows that observation of nucleating clusters in the atmosphere should be feasible. In the future, aircraft operation or measurements at high-altitude stations using CI-APi-TOF could provide insight into the importance of binary vs. ternary ammonia nucleation in the free troposphere.

Acknowledgements. We would like to thank CERN for supporting CLOUD with important technical and financial resources, and for providing a particle beam from the CERN Proton Synchrotron. This research was funded by the European Commission Seventh Framework Programme (Marie Curie Initial Training Network "CLOUD-ITN", grant no. 215072), the German Federal Ministry of Education and Research (project nos. 01LK0902A and 01LK1222A), the European Research Council Advanced Grant "ATMNUCLE" (project no. 227463), the Academy of Finland (project nos. 1133872, 1118615, and 272041), the Swiss National Science Foundation (project nos. 200020_135307 and 206620_141278), the US National Science Foundation (grants AGS-1439551 and AGS-1447056), the Austrian Science Fund (project nos. P19546 and L593), and the Davidow foundation. We thank the tofTools team for providing tools for mass spectrometry analysis.

Edited by: J. Abbatt

References

Almeida, J., Schobesberger, S., Kürten, A., Ortega, I. K., Kupiainen-Määttä, O., Praplan, A. P., Adamov, A., Amorim, A., Bianchi, F., Breitenlechner, M., David, A., Dommen, J., Donahue, N. M., Downard, A., Dunne, E. M., Duplissy, J., Ehrhart, S., Flagan, R. C., Franchin, A., Guida, R., Hakala, J., Hansel, A., Heinritzi, M., Henschel, H., Jokinen, T., Junninen, H., Kajos, M., Kangasluoma, J., Keskinen, H., Kupc, A., Kurtén, T., Kvashin, A. N., Laaksonen, A., Lehtipalo, K., Leiminger, M., Leppä, J., Loukonen, V., Makhmutov, V., Mathot, S., McGrath, M. J., Nieminen, T., Olenius, T., Onnela, A., Petäjä, T., Riccobono, F., Riipinen, I., Rissanen, M., Rondo, L., Ruuskanen, T., Santos, F. D., Sarnela, N., Schallhart, S., Schnitzhofer, R., Seinfeld, J. H., Simon, M., Sipilä, M., Stozhkov, Y., Stratmann, F., Tomé, A., Tröstl, J., Tsagkogeorgas, G., Vaattovaara, P., Viisanen, Y., Virtanen, A., Vrtala, A., Wagner, P. E., Weingartner, E., Wex, H., Williamson, C., Wimmer, D., Ye, P., Yli-Juuti, T., Carslaw, K. S., Kulmala, M., Curtius, J., Baltensperger, U., Worsnop, D. R., Vehkamäki, H., and Kirkby, J.: Molecular understanding of sulphuric acid-amine particle nucleation in the atmosphere, Nature, 502, 359–363, 2013.

Ball, S. M., Hanson, D. R., Eisele, F. L., and McMurry, P. H.: Laboratory studies of particle nucleation: Initial results for H_2SO_4, H_2O, and NH_3 vapors, J. Geophys. Res., 104, 23709–23718, doi:10.1029/1999JD900411, 1999.

Berresheim, H., Elste, T., Plass-Dülmer, C., Eisele, F. L., and Tanner, D. J.: Chemical ionization mass spectrometer for long-term measurements of atmospheric OH and H_2SO_4, Int. J. Mass Spectrom., 202, 91–109, 2000.

Bianchi, F., Dommen, J., Mathot, S., and Baltensperger, U.: Online determination of ammonia at low pptv mixing ratios in the CLOUD chamber, Atmos. Meas. Tech., 5, 1719–1725, doi:10.5194/amt-5-1719-2012, 2012.

Borrmann, S., Kunkel, D., Weigel, R., Minikin, A., Deshler, T., Wilson, J. C., Curtius, J., Volk, C. M., Homan, C. D., Ulanovsky, A., Ravegnani, F., Viciani, S., Shur, G. N., Belyaev, G. V., Law, K. S., and Cairo, F.: Aerosols in the tropical and subtropical UT/LS: in-situ measurements of submicron particle abundance and volatility, Atmos. Chem. Phys., 10, 5573–5592, doi:10.5194/acp-10-5573-2010, 2010.

Brock, C. A., Hamill, P., Wilson, J. C., Jonsson, H. H., and Chan, K. R.: Particle formation in the upper tropical troposphere: a source of nuclei for the stratospheric aerosol, Science, 270, 1650–1653, 1995.

Campbell, P. and Deshler, T.: Condensation nuclei measurements in the midlatitude (1982-2012) and Antarctic (1986-2010) stratosphere between 20 and 35 km, J. Geophys. Res., 119, 137–152, doi:10.1002/2013JD019710, 2014.

Chan, T. W. and Mozurkewich, M.: Measurement of the coagulation rate constant for sulfuric acid particles as a function of particle size using tandem differential mobility analysis, J. Aerosol Sci., 32, 321–339, 2001.

Chen, M., Titcombe, M., Jiang, J., Jen, C., Kuang, C., Fischer, M. L., Eisele, F. L., Siepmann, J. I., Hanson, D. R., Zhao, J., and McMurry, P. H.: Acid–base chemical reaction model for nucleation rates in the polluted atmospheric boundary layer, P. Natl. Acad. Sci. USA, 109, 18713–18718, doi:10.1073/pnas.1210285109, 2012.

Chon, N. L., Lee, S.-H., and Lin, H.: A theoretical study of temperature dependence of cluster formation from sulfuric acid and ammonia, Chem. Phys., 433, 60–66, 2014.

Clarke, A. D., Eisele, F., Kapustin, V. N., Moore, K., Tanner, D., Mauldin, L., Litchy, M., Lienert, B., Carroll, M. A., and Albercook, G.: Nucleation in the equatorial free troposphere: favorable environments during PEM-Tropics, J. Geophys. Res., 104, 5735–5744, 1999.

Curtius, J., Froyd, K. D., and Lovejoy, E. R.: Cluster ion thermal decomposition (I): Experimental kinetics study and ab initio calculations for $HSO_4^-(H_2SO_4)_x(HNO_3)_y$, J. Phys. Chem. A, 105, 10867–10873, 2001.

Ding, C.-G., Laasonen, K., and Laaksonen, A.: Two sulfuric acids in small water clusters, J. Phys. Chem. A, 107, 8648–8658, 2003.

Duplissy, J., Enghoff, M. B., Aplin, K. L., Arnold, F., Aufmhoff, H., Avngaard, M., Baltensperger, U., Bondo, T., Bingham, R., Carslaw, K., Curtius, J., David, A., Fastrup, B., Gagné, S., Hahn, F., Harrison, R. G., Kellett, B., Kirkby, J., Kulmala, M., Laakso,

L., Laaksonen, A., Lillestol, E., Lockwood, M., Mäkelä, J., Makhmutov, V., Marsh, N. D., Nieminen, T., Onnela, A., Pedersen, E., Pedersen, J. O. P., Polny, J., Reichl, U., Seinfeld, J. H., Sipilä, M., Stozhkov, Y., Stratmann, F., Svensmark, H., Svensmark, J., Veenhof, R., Verheggen, B., Viisanen, Y., Wagner, P. E., Wehrle, G., Weingartner, E., Wex, H., Wilhelmsson, M., and Winkler, P. M.: Results from the CERN pilot CLOUD experiment, Atmos. Chem. Phys., 10, 1635–1647, doi:10.5194/acp-10-1635-2010, 2010.

Duplissy, J., Merikanto, J., Franchin, A., Tsagkogeorgas, G., Kangasluoma, J., Wimmer, D., Vuollekoski, H., Schobesberger, S., Lehtipalo, K., Flagan, R. C., Brus, D., Donahue, N. M., Vehkämäki, H., Almeida, J., Amorim, A., Barmet, P., Bianchi, F., Breitenlechner, M., Dunne, E. M., Guida, R., Henschel, H., Junninen, H., Kirkby, J., Kürten, A., Kupc, A., Määttänen, A., Makhmutov, V., Mathot, S. , Nieminen, T., Onnela, A., Praplan, A. P., Riccobono, F., Rondo, L., Steiner, G., Tome, A., Walther, H., Baltensperger, U., Carslaw, K. S., Dommen, J., Hansel, A., Petäjä, T., Sipilä, M., Stratmann, F., Vrtala, A., Wagner, P. E., Worsnop, D. R., Curtius, J., and Kulmala, M.: Effect of ions on sulfuric acid-water binary particle formation II: Experimental data and comparison with QC-normalized classical nucleation theory, J. Geophys. Res.-Atmos., 120, doi:10.1002/2015JD023539, 2015.

Ehrhart, S. and Curtius, J.: Influence of aerosol lifetime on the interpretation of nucleation experiments with respect to the first nucleation theorem, Atmos. Chem. Phys., 13, 11465–11471, doi:10.5194/acp-13-11465-2013, 2013.

Eisele, F. L. and Hanson, D. R.: First measurement of prenucleation molecular clusters, J. Phys. Chem. A, 104, 830–836, 2000.

Eisele, F. L. and Tanner, D. J.: Measurement of the gas phase concentration of H_2SO_4 and methane sulfonic acid and estimates of H_2SO_4 production and loss in the atmosphere, J. Geophys. Res., 98, 9001–9010, 1993.

Eisele, F. L., Lovejoy, E. R., Kosciuch, E., Moore, K. F., Mauldin III, R. L., Smith, J. N., McMurry, P. H., and Iida, K.: Negative atmospheric ions and their potential role in ion-induced nucleation, J. Geophys. Res., 111, D04305, doi:10.1029/2005JD006568, 2006.

Franchin, A., Ehrhart, S., Leppä, J., Nieminen, T., Gagné, S., Schobesberger, S., Wimmer, D., Duplissy, J., Riccobono, F., Dunne, E. M., Rondo, L., Downard, A., Bianchi, F., Kupc, A., Tsagkogeorgas, G., Lehtipalo, K., Manninen, H. E., Almeida, J., Amorim, A., Wagner, P. E., Hansel, A., Kirkby, J., Kürten, A., Donahue, N. M., Makhmutov, V., Mathot, S., Metzger, A., Petäjä, T., Schnitzhofer, R., Sipilä, M., Stozhkov, Y., Tomé, A., Kerminen, V.-M., Carslaw, K., Curtius, J., Baltensperger, U., and Kulmala, M.: Experimental investigation of ion-ion recombination under atmospheric conditions, Atmos. Chem. Phys., 15, 7203–7216, doi:10.5194/acp-15-7203-2015, 2015.

Froyd, K. D. and Lovejoy, E. R.: Experimental thermodynamics of cluster ions composed of H_2SO_4 and H_2O. 2. Measurements and ab initio structures of negative ions, J. Phys. Chem. A, 107, 9812–9824, 2003.

Hanson, D. R. and Eisele, F.: Diffusion of H_2SO_4 in humidified nitrogen: hydrated H_2SO_4, J. Phys. Chem. A, 104, 1715–1719, 2000.

Hanson, D. R. and Eisele, F. L.: Measurement of prenucleation molecular clusters in the NH_3, H_2SO_4, H_2O system, J. Geophys. Res., 107, 4158, doi:10.1029/2001JD001100, 2002.

Hanson, D. R. and Lovejoy, E. R.: Measurement of the thermodynamics of the hydrated dimer and trimer of sulfuric acid, J. Phys. Chem. A, 110, 9525–9528, 2006.

Henschel, H., Navarro, J. C. A., Yli-Juuti, T., Kupiainen-Määttä, O., Olenius, T., Ortega, I. K., Clegg, S. L., Kurtén, T., Riipinen, I., and Vehkamäki, H.: Hydration of Atmospherically Relevant Molecular Clusters: Computational Chemistry and Classical Thermodynamics, J. Phys. Chem. A, 118, 2599–2611, 2014.

Herb, J., Nadykto, A. B., and Yu, F.: Large ternary hydrogen-bonded pre-nucleation clusters in the Earth's atmosphere, Chem. Phys. Lett., 518, 7–14, 2011.

Jen, C., McMurry, P. H., and Hanson, D. R.: Stabilization of sulfuric acid dimers by ammonia, methylamine, dimethylamine, and trimethylamine, J. Geophys. Res.-Atmos., 119, 7502–7514, doi:10.1002/2014JD021592, 2014.

Jokinen, T., Sipilä, M., Junninen, H., Ehn, M., Lönn, G., Hakala, J., Petäjä, T., Mauldin III, R. L., Kulmala, M., and Worsnop, D. R.: Atmospheric sulphuric acid and neutral cluster measurements using CI-APi-TOF, Atmos. Chem. Phys., 12, 4117–4125, doi:10.5194/acp-12-4117-2012, 2012.

Junninen, H., Ehn, M., Petäjä, T., Luosujärvi, L., Kotiaho, T., Kostiainen, R., Rohner, U., Gonin, M., Fuhrer, K., Kulmala, M., and Worsnop, D. R.: A high-resolution mass spectrometer to measure atmospheric ion composition, Atmos. Meas. Tech., 3, 1039–1053, doi:10.5194/amt-3-1039-2010, 2010.

Kanawade, V. and Tripathi, S. N.: Evidence for the role of ion-induced particle formation during an atmospheric nucleation event observed in Tropospheric Ozone Production about the Spring Equinox (TOPSE), J. Geophys. Res., 111, D02209, doi:10.1029/2005JD006366, 2006.

Kazil, J. and Lovejoy, E. R.: A semi-analytical method for calculating rates of new sulfate aerosol formation from the gas phase, Atmos. Chem. Phys., 7, 3447–3459, doi:10.5194/acp-7-3447-2007, 2007.

Kerminen, V.-M., Petäjä, T., Manninen, H. E., Paasonen, P., Nieminen, T., Sipilä, M., Junninen, H., Ehn, M., Gagné, S., Laakso, L., Riipinen, I., Vehkamäki, H., Kurten, T., Ortega, I. K., Dal Maso, M., Brus, D., Hyvärinen, A., Lihavainen, H., Leppä, J., Lehtinen, K. E. J., Mirme, A., Mirme, S., Hõrrak, U., Berndt, T., Stratmann, F., Birmili, W., Wiedensohler, A., Metzger, A., Dommen, J., Baltensperger, U., Kiendler-Scharr, A., Mentel, T. F., Wildt, J., Winkler, P. M., Wagner, P. E., Petzold, A., Minikin, A., Plass-Dülmer, C., Pöschl, U., Laaksonen, A., and Kulmala, M.: Atmospheric nucleation: highlights of the EUCAARI project and future directions, Atmos. Chem. Phys., 10, 10829–10848, doi:10.5194/acp-10-10829-2010, 2010.

Kirkby, J., Curtius, J., Almeida, J., Dunne, E., Duplissy, J., Ehrhart, S., Franchin, A., Gagné, S., Ickes, L., Kürten, A., Kupc, A., Metzger, A., Riccobono, F., Rondo, L., Schobesberger, S., Tsagkogeorgas, G., Wimmer, D., Amorim, A., Bianchi, F., Breitenlechner, M., David, A., Dommen, J., Downard, A., Ehn, M., Flagan, R.C., Haider, S., Hansel, A., Hauser, D., Jud, W., Junninen, H., Kreissl, F., Kvashin, A., Laaksonen, A., Lehtipalo, K., Lima, J., Lovejoy, E. R., Makhmutov, V., Mathot, S., Mikkilä, J., Minginette, P., Mogo, S., Nieminen, T., Onnela, A., Pereira, P., Petäjä, T., Schnitzhofer, R., Seinfeld, J. H., Sipilä, M., Stozhkov, Y., Strat-

mann, F., Tomé, A., Vanhanen, J., Viisanen, Y., Vrtala, A., Wagner, P. E., Walther, H., Weingartner, E., Wex, H., Winkler, P. M., Carslaw, K. S., Worsnop, D. R., Baltensperger, U., and Kulmala, M.: Role of sulphuric acid, ammonia and galactic cosmic rays in atmospheric aerosol nucleation, Nature, 476, 429–435, 2011.

Kuang, C., McMurry, P. H., McCormick, A. V., and Eisele, F. L.: Dependence of nucleation rates on sulfuric acid vapor concentration in diverse atmospheric locations, J. Geophys. Res., 113, D10209, doi:10.1029/2007JD009253, 2008.

Kulmala, M., Vehkamäki, H., Petäjä, T., Dal Maso, M., Lauri, A., Kerminen, V.-M., Birmili, W., and McMurry, P. H.: Formation and growth rates of ultrafine atmospheric particles: a review of observations, J. Aerosol Sci., 35, 143–176, 2004.

Kulmala, M., Kontkanen, J., Junninen, H., Lehtipalo, K., Manninen, H. E., Nieminen, T., Petäjä, T., Sipilä, M., Schobesberger, S., Rantala, P., Franchin, A., Jokinen, T., Järvinen, E., Äijälä, M., Kangasluoma, J., Hakala, J., Aalto, P. P., Paasonen, P., Mikkilä, J., Vanhanen, J., Aalto, J., Hakola, H., Makkonen, U., Ruuskanen, T., Mauldin III, R. L., Duplissy, J., Vehkamäki, H., Bäck, J., Kortelainen, A., Riipinen, I., Kurtén, T., Johnston, M. V., Smith, J. N., Ehn, M., Mentel, T. F., Lehtinen, K. E. J., Laaksonen, A., Kerminen, V.-M., and Worsnop, D. R.: Direct observations of atmospheric aerosol nucleation, Science, 339, 943–946, doi:10.1126/science.1227385, 2013.

Kupc, A., Amorim, A., Curtius, J., Danielczok, A., Duplissy, J., Ehrhart, S., Walther, H., Ickes, L., Kirkby, J., Kürten, A., Lima, J. M., Mathot, S., Minginette, P., Onnela, A., Rondo, L., and Wagner, P. E.: A fibre-optic UV system for H_2SO_4 production in aerosol chambers causing minimal thermal effects, J. Aerosol Sci., 42, 532–543, 2011.

Kupiainen-Määttä, O., Olenius, T., Kurtén, T., and Vehkamäki, H.: CIMS sulfuric acid detection efficiency enhanced by amines due to higher dipole moments: a computational study, J. Phys. Chem. A, 117, 14109–14119, 2013.

Kürten, A., Rondo, L., Ehrhart, S., and Curtius, J.: Performance of a corona ion source for measurement of sulfuric acid by chemical ionization mass spectrometry, Atmos. Meas. Tech., 4, 437–443, doi:10.5194/amt-4-437-2011, 2011.

Kürten, A., Rondo, L., Ehrhart, S., and Curtius, J.: Calibration of a chemical ionization mass spectrometer for the measurement of gaseous sulfuric acid, J. Phys. Chem. A, 116, 6375–6386, doi:10.1021/jp212123n, 2012.

Kürten, A., Jokinen, T., Simon, M., Sipilä, M., Sarnela, N., Junninen, H., Adamov, A., Almeida, J., Amorim, A., Bianchi, F., Breitenlechner, M., Dommen, J., Donahue, N. M., Duplissy, J., Ehrhart, S., Flagan, R. C., Franchin, A., Hakala, J., Hansel, A., Heinritzi, M., Hutterli, M., Kangasluoma, J., Kirkby, J., Laaksonen, A., Lehtipalo, K., Leiminger, M., Makhmutov, V., Mathot, S., Onnela, A., Petäjä, T., Praplan, A. P., Riccobono, F., Rissanen, M. P., Rondo, L., Schobesberger, S., Seinfeld, J. H., Steiner, G., Tomé, A., Tröstl, J., Winkler, P. M., Williamson, C., Wimmer, D., Ye, P., Baltensperger, U., Carslaw, K. S., Kulmala, M., Worsnop, D. R., and Curtius, J.: Neutral molecular cluster formation of sulfuric acid-dimethylamine observed in real-time under atmospheric conditions, P. Natl. Acad. Sci. USA, 111, 15019–15024, doi:10.1073/pnas.1404853111, 2014.

Kurtén, T., Torpo, L., Ding, C.-G., Vehkamäki, H., Sundberg, M. R., Laasonen, K., and Kulmala, M.: A density functional study on water-sulfuric acid-ammonia clusters and implications for atmospheric cluster formation, J. Geophys. Res., 112, D04210, doi:10.1029/2006JD007391, 2007.

Kurtén, T., Petäjä, T., Smith, J., Ortega, I. K., Sipilä, M., Junninen, H., Ehn, M., Vehkamäki, H., Mauldin, L., Worsnop, D. R., and Kulmala, M.: The effect of H_2SO_4 – amine clustering on chemical ionization mass spectrometry (CIMS) measurements of gas-phase sulfuric acid, Atmos. Chem. Phys., 11, 3007–3019, doi:10.5194/acp-11-3007-2011, 2011.

Lee, S.-H., Reeves, J. M., Wilson, J. C., Hunton, D. E., Viggiano, A. A., Miller, T. M., Ballenthin, J. O., and Lait, L. R.: Particle formation by ion nucleation in the upper troposphere and lower stratosphere, Science, 301, 1886–1889, doi:10.1126/science.1087236, 2003.

Lovejoy, E. R. and Curtius, J.: Cluster ion thermal decomposition (II): Master equation modeling in the low-pressure limit and fall-off regions. Bond energies for $HSO_4^-(H_2SO_4)_x(HNO_3)_y$, J. Phys. Chem. A, 105, 10874–10883, 2001.

Lovejoy, E. R., Curtius, J., and Froyd, K. D.: Atmospheric ion-induced nucleation of sulfuric acid and water, J. Geophys. Res., 109, D08204, doi:10.1029/2003JD004460, 2004.

Mauldin, R. L., Tanner, D. J., Heath, J. A., Huebert, B. J., and Eisele, F. L.: Observations of H_2SO_4 and MSA during PEM-Tropics-A, J. Geophys. Res., 104, 5801–5816, 1999.

McMurry, P. H.: Photochemical Aerosol Formation from SO_2: A theoretical analysis of smog chamber data, J. Colloid Interf. Sci., 78, 513–527, 1980.

Murphy, D. M. and Koop, T.: Review of the vapour pressures of ice and supercooled water for atmospheric applications, Q. J. Roy. Meteorol. Soc., 131, 1539–1565, 2005.

Nadykto, A. B. and Yu, F.: Strong hydrogen bonding between atmospheric nucleation precursors and common organics, Chem. Phys. Lett., 435, 14–18, 2007.

Norman, M., Hansel, A., and Wisthaler, A.: O_2^+ as reagent ion in the PTR-MS instrument: detection of gas-phase ammonia, Int. J. Mass Spectrom., 265, 382–387, 2007.

Ortega, I. K., Kupiainen, O., Kurtén, T., Olenius, T., Wilkman, O., McGrath, M. J., Loukonen, V., and Vehkamäki, H.: From quantum chemical formation free energies to evaporation rates, Atmos. Chem. Phys., 12, 225–235, doi:10.5194/acp-12-225-2012, 2012.

Ortega, I. K., Olenius, T., Kupiainen-Määttä, O., Loukonen, V., Kurtén, T., and Vehkamäki, H.: Electrical charging changes the composition of sulfuric acid-ammonia/dimethylamine clusters, Atmos. Chem. Phys., 14, 7995–8007, doi:10.5194/acp-14-7995-2014, 2014.

Paasonen, P., Olenius, T., Kupiainen, O., Kurtén, T., Petäjä, T., Birmili, W., Hamed, A., Hu, M., Huey, L. G., Plass-Duelmer, C., Smith, J. N., Wiedensohler, A., Loukonen, V., McGrath, M. J., Ortega, I. K., Laaksonen, A., Vehkamäki, H., Kerminen, V.-M., and Kulmala, M.: On the formation of sulphuric acid – amine clusters in varying atmospheric conditions and its influence on atmospheric new particle formation, Atmos. Chem. Phys., 12, 9113–9133, doi:10.5194/acp-12-9113-2012, 2012.

Petäjä, T., Sipilä, M., Paasonen, P., Nieminen, T., Kurtén, T., Ortega, I. K., Stratmann, F., Vehkamäki, H., Berndt, T., and Kulmala, M.: Experimental observation of strongly bound dimers of sulfuric acid: application to nucleation in the atmosphere, Phys. Rev. Lett., 106, 228302-1–228302-4, 2011.

Praplan, A. P., Bianchi, F., Dommen, J., and Baltensperger, U.: Dimethylamine and ammonia measurements with ion chromatography during the CLOUD4 campaign, Atmos. Meas. Tech., 5, 2161–2167, doi:10.5194/amt-5-2161-2012, 2012.

Riccobono, F., Schobesberger, S., Scott, C. E., Dommen, J., Ortega, I. K., Rondo, L., Almeida, J., Amorim, A., Bianchi, F., Breitenlechner, M., David, A., Downard, A., Dunne, E. M., Duplissy, J., Ehrhart, S., Flagan, R. C., Franchin, A., Hansel, A., Junninen, H., Kajos, M., Keskinen, H., Kupc, A., Kürten, A., Kvashin, A. N., Laaksonen, A., Lehtipalo, K., Makhmutov, V., Mathot, S., Nieminen, T., Onnela, A., Petäjä, T., Praplan, A. P., Santos, F. D., Schallhart, S., Seinfeld, J. H., Sipilä, M., Spracklen, D. V., Stozhkov, Y., Stratmann, F., Tomé, A., Tsagkogeorgas, G., Vaattovaara, P., Viisanen, Y., Vrtala, A., Wagner, P. E., Weingartner, E., Wex, H., Wimmer, D., Carslaw, K. S., Curtius, J., Donahue, N. M., Kirkby, J., Kulmala, M., Worsnop, D. R., and Baltensperger, U.: Oxidation products of biogenic emissions contribute to nucleation of atmospheric particles, Science, 344, 717–721, 2014.

Rondo, L., Kürten, A., Ehrhart, S., Schobesberger, S., Franchin, A., Junninen, H., Petäjä, T., Sipilä, M., Worsnop, D. R., and Curtius, J.: Effect of ions on the measurement of sulfuric acid in the CLOUD experiment at CERN, Atmos. Meas. Tech., 7, 3849–3859, doi:10.5194/amt-7-3849-2014, 2014.

Rondo, L., Ehrhart, S., Kürten, A., Adamov, A., Bianchi, F., Breitenlechner, M., Duplissy, J., Franchin, A., Dommen, J., Donahue, N. M., Dunne, E. M., Flagan, R. C., Hakala, J., Hansel, A., Keskinen, H., Kim, J., Jokinen, T., Lehtipalo, K., Leiminger, M., Praplan, A., Riccobono, F., Rissanen, M. P., Sarnela, N., Schobesberger, S., Simon, M., Sipilä, M., Smith, J. N., Tomé, A., Tröstl, J., Tsagkogeorgas, G., Vaattovaara, P., Winkler, P. M., Williamson, C., Baltensperger, U., Kirkby, J., Kulmala, M., Worsnop, D. R., and Curtius, J.: Effect of dimethylamine on the gas phase sulfuric acid concentration measured by Chemical Ionization Mass Spectrometry (CIMS), J. Geophys. Res., submitted, 2015.

Sceats, M. G.: Brownian coagulation in aerosols–The role of long range forces, J. Colloid Interf. Sci., 129, 105–112, 1989.

Schobesberger, S., Junninen, H., Bianchi, F., Lönn, G., Ehn, M., Lehtipalo, K., Dommen, J., Ehrhart, S., Ortega, I. K., Franchin, A., Nieminen, T., Riccobono, F., Hutterli, M., Duplissy, J., Almeida, J., Amorim, A., Breitenlechner, M., Downard, A. J., Dunne, E. M., Flagan, R. C., Kajos, M., Keskinen, H., Kirkby, J., Kupc, A., Kürten, A., Kurtén, T., Laaksonen, A., Mathot, S., Onnela, A., Praplan, A. P., Rondo, L., Santos, F. D., Schallhart, S., Schnitzhofer, R., Sipilä, M., Tomé, A., Tsagkogeorgas, G., Vehkamäki, H., Wimmer, D., Baltensperger, U., Carslaw, K. S., Curtius, J., Hansel, A., Petäjä, T., Kulmala, M., Donahue, N. M., and Worsnop, D. R.: Molecular understanding of atmospheric particle formation from sulfuric acid and large oxidized organic molecules, P. Natl. Acad. Sci. USA, 110, 17223–17228, doi:10.1073/pnas.1306973110, 2013.

Schobesberger, S., Franchin, A., Bianchi, F., Rondo, L., Duplissy, J., Kürten, A., Ortega, I. K., Metzger, A., Schnitzhofer, R., Almeida, J., Amorim, A., Dommen, J., Dunne, E. M., Ehn, M., Gagné, S., Ickes, L., Junninen, H., Hansel, A., Kerminen, V.-M., Kirkby, J., Kupc, A., Laaksonen, A., Lehtipalo, K., Mathot, S., Onnela, A., Petäjä, T., Riccobono, F., Santos, F. D., Sipilä, M., Tomé, A., Tsagkogeorgas, G., Viisanen, Y., Wagner, P. E., Wimmer, D., Curtius, J., Donahue, N. M., Baltensperger, U., Kulmala, M., and Worsnop, D. R.: On the composition of ammonia-sulfuric-acid ion clusters during aerosol particle formation, Atmos. Chem. Phys., 15, 55–78, doi:10.5194/acp-15-55-2015, 2015.

Temelso, B., Phan, T. N., and Shields, G. C.: Computational Study of the Hydration of Sulfuric Acid Dimers: Implications for Acid Dissociation and Aerosol Formation, J. Phys. Chem. A, 116, 9745–9758, 2012.

Torpo, L., Kurtén, T., Vehkamäki, H., Laasonen, K., Sundberg, M. R., and Kulmala, M.: Significance of ammonia in growth of atmospheric nanoclusters, J. Phys. Chem. A, 111, 10671–10674, 2007.

Viggiano, A. A., Dale, F., and Paulson, J. F.: Measurements of some stratospheric ion-molecule association rates: Implications for ion chemistry and derived HNO_3 concentrations in the stratosphere, J. Geophys. Res.-Atmos., 90, 7977–7984, doi:10.1029/JD090iD05p07977, 1985.

Viggiano, A. A., Seeley, J. V., Mundis, P. L., Williamson, J. S., and Morris, R. A.: Rate constants for the reactions of $XO_3^-(H_2O)_n$(X = C, HC, and N) and $NO_3^-(HNO_3)_n$with H_2SO_4: implications for atmospheric detection of H_2SO_4, J. Phys. Chem. A, 101, 8275–8278, 1997.

Voigtländer, J., Duplissy, J., Rondo, L., Kürten, A., and Stratmann, F.: Numerical simulations of mixing conditions and aerosol dynamics in the CERN CLOUD chamber, Atmos. Chem. Phys., 12, 2205–2214, doi:10.5194/acp-12-2205-2012, 2012.

Weber, R. J., McMurry, P. H., Eisele, F. L., and Tanner, D. J.: Measurement of expected nucleation precursor species and 3-500-nm diameter particles at Mauna Loa observatory, Hawaii, J. Atmos. Sci., 52, 2242–2257, 1995.

Weber, R., McMurry, P. H., Mauldin, L., Tanner, D. J., Eisele, F. L., Brechtel, F. J., Kreidenweis, S. M., Kok, G., Schillawski, R. D., and Baumgardner, D.: A study of new particle formation and growth involving biogenic and trace gas species measured during ACE 1, J. Geophys. Res., 103, 16385–16396, 1998.

Weigel, R., Borrmann, S., Kazil, J., Minikin, A., Stohl, A., Wilson, J. C., Reeves, J. M., Kunkel, D., de Reus, M., Frey, W., Lovejoy, E. R., Volk, C. M., Viciani, S., D'Amato, F., Schiller, C., Peter, T., Schlager, H., Cairo, F., Law, K. S., Shur, G. N., Belyaev, G. V., and Curtius, J.: In situ observations of new particle formation in the tropical upper troposphere: the role of clouds and the nucleation mechanism, Atmos. Chem. Phys., 11, 9983–10010, doi:10.5194/acp-11-9983-2011, 2011.

Zhang, R., Khalizov, A., Wang, L., Hu, M., and Xu, W.: Nucleation and growth of nanoparticles in the atmosphere, Chem. Rev., 112, 1957–2011, 2012.

Zhao, J., Eisele, F. L., Titcombe, M., Kuang, C., and McMurry, P. H.: Chemical ionization mass spectrometric measurements of atmospheric neutral clusters using the cluster-CIMS, J. Geophys. Res., 115, D08205, doi:10.1029/2009JD012606, 2010.

Zollner, J. H., Glasoe, W. A., Panta, B., Carlson, K. K., McMurry, P. H., and Hanson, D. R.: Sulfuric acid nucleation: power dependencies, variation with relative humidity, and effect of bases, Atmos. Chem. Phys., 12, 4399–4411, doi:10.5194/acp-12-4399-2012, 2012.